A Survey of Topology-based Methods in Visualization

C. Heine[1], H. Leitte[1], M. Hlawitschka[2], F. Iuricich[3], L. De Floriani[4], G. Scheuermann[5], H. Hagen[1], and C. Garth[1]

[1]Department of Computer Science, University of Kaiserslautern, Germany
[2]Faculty for Computer Science, HTWK Leipzig, Germany
[3]University of Maryland, College Park (MD), USA
[4]DIBRIS, University of Genoa, Italy
[5]Institute for Computer Science, University of Leipzig, Germany

Abstract
This paper presents the state of the art in the area of topology-based visualization. It describes the process and results of an extensive annotation for generating a definition and terminology for the field. The terminology enabled a typology for topological models which is used to organize research results and the state of the art. Our report discusses relations among topological models and for each model describes research results for the computation, simplification, visualization, and application. The paper identifies themes common to subfields, current frontiers, and unexplored territory in this research area.

1. Introduction

Topology-based visualization has established itself as a versatile approach to analyze scientific data. But beginners and experts alike find it increasingly difficult to navigate the enormous body of literature on the topic. In this paper, we report on a study of the relevant literature to clearly delimit and organize the field, and discuss recent research results and trends. The contributions of this paper are:

- we propose a definition for topology-based visualization that is as of yet been lacking in the literature,
- an organized and, in part, homogenized terminology for the relevant concepts, and
- an overview of important research results in the field, identifying current challenges and problems.

This report is intended for experts in the field seeking an up-to-date overview or looking for synergies and unmet challenges, as well as beginners and general visualization researchers interested in the current state and capabilities of topology-based visualization.

The most similar predecessor to our paper is the survey on flow field topology by Laramee et al. [LHZP07]. It contains a typology for topology-based visualization, which, similar to ours, also uses the separation of scalar, vector, and tensor field as well as time-independent and time-dependent. Our classification considers developments in multifields and uncertainty visualization in addition. The survey by Laramee et al. classified but did not elaborate on scalar and tensor fields. The recent survey by Wang et al. [WWL16] also focuses on vector field topology exclusively. The surveys by Biasotti et al. [BGSF08,BDF*08] and De Floriani et al. [DFFIM15] cover topological models for scalar fields, but focus on shape description applications rather than visualization. The surveys on

time-dependent isosurfaces [MS09], feature tracking [PVH*03], multifields [FH09], and high-dimensional data [LMW*15] cover some topological methods, but even jointly they cover only a subset of this state-of-the-art report's scope. Our larger scope prohibits an exhaustive discussion of the field's results; instead we emphasize more recent and visualization-targeted papers.

In this report, we first briefly describe the literature collection and annotation process underlying our work, define the term "topology-based visualization" and give a typology of topological models for visualization. We will then describe research results related to each of the topological models in an order supported by the typology and finish with a discussion of similarities and differences among topology-based methods for different classes of data.

2. Literature Research Procedure & Classification

We compiled an initial set of papers from the authors' literature databases on the topic. In a first phase, this compilation was read, annotated, and judged for typicality – the later was to shape a definition for topology-based visualization; there is not yet one in print. The purpose of the annotation was to construct a terminology suitable to group papers and thus organize the field. The annotation was guided by a list of aspects to look out for (e.g., application area, input data type, serial vs. parallel). As a side-product we noted synonyms for structurally identical concepts. Even though the initial set of papers did not fully cover the field, we deemed the selection to be representative enough to meet these two goals.

We then analyzed the results of this first annotation phase, to construct a definition of topology-based visualization:

> Topology-based visualization uses topological concepts

to describe, reduce, or organize data in order to be used in visualization. Typical topological concepts are, e.g., topological space, cell complex, homotopy equivalence, homology, connectedness, quotient space. Typical visualization uses are, e.g. to highlight data subsets, to provide a structural overview, or to guide interactive exploration.

Successively, we took the list of keywords resulting from the first annotation, grouped them by aspect, replaced infrequent terms of the same aspect by hyperonyms, sharpened ambiguous terms, organized the terms of each aspect hierarchically, and added terms to complement aspects, i.e. to ensure each paper can be categorized with respect to any aspect. The annotations were very helpful in discussing and establishing clear definitions for the classes.

Before the second phase, we added papers from recent years of journals TVCG and CGF as well as proceedings of the VIS, EuroVis, PacificVis, and LDAV conferences plus the Topology in Visualization workshops when they met our definition for topology-based visualization, as judged from title and abstract. Given our focus on topological methods with applications in visualization, we did not explicitly consider computational geometry journals and conference proceedings. We also removed papers from the initial collection that did not meet our definition. In the second phase, we then went through all these papers and categorized them again using a questionnaire form constructed from our refined terminology. We allowed for the addition of comments to each aspect of categorization to enabling adding terms we missed before. As it turns out, this was hardly ever necessary; it was more often used to elaborate on a term or note a synonym. Each paper was categorized by at least one person. The first round annotations were used to check for consistency. If a paper's related work pointed to other potentially relevant papers, they were again checked against our relevance criterion and added to the corpus for processing if relevant. In total, this report is based on a survey of approximately 350 publications.

Our annotation resulted in a classification along multiple axes, not necessarily independent, plus some optional labels. The first axis pertaining to input data is the *input class* with the following options: a *scalar field* represents a real-valued function, a *vector field* represents a vector-valued function, a *tensor field* represents a tensor-valued function, and a *multifield* is a collection of functions of any type on the same domain. Neither vector nor tensor fields are treated as multiple scalar fields, instead we take multifield to refer to fields of different modality, e.g., pressure and density in physical simulations. Instead, if there is an ensemble of fields arising from varying simulation parameters, the axis *parameters* denotes their number. Input data may be labeled *uncertain*, when, e.g., it is given as a probability distribution over the set of all functions or as a set of samples drawn from a distribution over functions.

Since all our objects of study are functions, two axes describe the domain of the function more closely. The first gives the *input's topological dimension* (e.g., surfaces have topological dimension 2). We did not consider the geometric dimension, i.e. the dimension of the space the function's domain is embedded in, because it has no effect on topological properties of the function. In addition, the function may be labeled *time-independent* or *time-dependent*. We distinguish time from space, rather than just increasing the space dimension, because time and space have idiosyncratic meanings.

Finally, the function has to be stored using a finite data structure to be amenable to computational processing. The *domain discretization* can be either *piecewise constant*, *piecewise linear* (simplicial cells), *structured* (regular arrangement of (hyper-)cubical cells), *unstructured*, or *combinatorial* (special case for discrete Morse theory). We did not come across any topological methods for meshless, e.g. SPH, data. We did not consider the interpolation of the spatial embedding since it does not affect topology.

Our core axis of classification, having the most classes, is the *topological model* of the function(s). For scalar fields we have *critical points*; *persistent homology*; level-set-based approaches like *merge tree*, *contour tree*, and *Reeb graph*; and gradient-based approaches like the *Morse-Smale complex*. For vector fields we have *critical points*, *invariant sets*, *separatrices*, *saddle connectors*, *Morse complex*, *FTLE/LCS*, and *Morse decomposition*. Within tensor fields we have *degenerate points/lines* and *separatrices*. Within multifields we distinguish between *Jacobi sets*, *Reeb space*, *joint contour net*, and *Pareto sets*. We also noted whether research results made use of *topological simplification* for removal of topological features and whether it is driven by *persistence* – the maximum change to a function to remove the feature, *size* – the domain subset covered by the feature, *energy* – the total amount of change to a function to remove the feature, *scale space*, or *other* methods.

Concerning the computation we annotated whether the *algorithmic strategy* is primarily *numerical*, i.e., solves ordinary differential equations or large linear systems; *combinatorial*, i.e., mostly uses comparisons and branching; or *statistical*, i.e., computes averages, variances, or confidence intervals. We also considered the *mode of computation*, i.e., whether it was declared by the authors as *concurrent*, *data-parallel*, or *distributed*. We noted when an algorithm was declared *approximate*, whether it uses a *divide-and-conquer* strategy, and whether it is *streaming*, i.e., able to process data while it arises. Further labels taken from the original works are *memory-efficient*, when the amount of memory required is kept small, *out-of-core*, when parts of the data can be left on disk, and *I/O-efficient*, when disk access is minimized in addition.

Finally, the *visualization use* considers how the topological structure is employed within the surrounding visualization. Possible uses are *highlighting* if the topological structure is shown by marking or coloring points in the original function's domain. It can also *guide representation*, e.g. via topology-controlled volume rendering or seeding integration lines and surfaces, Topological structure can also be *metaphorically represented*, e.g., via graph drawing or topological landscapes. The topological structure is sometimes also used to *guide interaction*, e.g. inform manual selection of isosurfaces or present the data at multiple levels of detail after topological simplification gave rise to feature importance. Another use relevant to time-dependent data is *feature identification & tracking*, and an upcoming topic is the topology-controlled *compression* of data for in-situ analysis. We also annotated the *application domain* of the topology-based visualization, but the resulting classes are small and too numerous to list here.

After annotation we noticed that the classification axes *input class*, *uncertainty*, and *time-dependency* jointly determine the type of topological model and can therefore be used to construct a typology of topological models, presented in Table 1.

Table 1: *Typology of Topological Models*

	certain		uncertain	
	time-independent	time-dependent	time-independent	time-dependent
scalar	critical points, persistent homology, merge tree, contour tree, Reeb graph, Morse-Smale complex, extremum graph	critical point tracking, dynamic merge tree, dynamic contour tree	mandatory critical points, critical point confidence region	
vector	critical points, invariant sets, separatrices, saddle connectors, Morse decomposition	critical point tracking, LCS, streak line topology, unsteady vector field topology	stable Morse decomposition, uncertain vector field toplogy	uncertain LCS
tensor	degenerate points & lines, separatrices	tensor topology tracking		
multi	Jacobi set, Reeb space joint contour net, Pareto sets			

3. State of the Art – Scalar Fields

There is a plethora of topological models for scalar fields. We note that models for time-dependent/uncertain data are often dynamic/statistical extensions to the time-independent/certain case. We will survey the base case first and then describe the extensions.

3.1. Certain Time-Independent Scalar Fields

Most topology-based visualizations for certain time-independent scalar fields build on Morse theory for real-valued functions defined on manifolds, in particular critical points and their relations.

3.1.1. Critical Points and Persistent Homology

A *critical point* of a function $f : \mathbb{M} \to \mathbb{R}$ is a point p at which the gradient of f vanishes: $\nabla f(p) = \mathbf{0}$; all other points of the d-manifold $\mathbb{M}$ are called *regular* or *ordinary*. A critical point p is *degenerate* if the *Hessian*, i.e., the matrix of second-order derivatives $H_{i,j} = \frac{\partial^2 f}{\partial x_i \partial x_j}$ is singular at p. A smooth function f is called *Morse* if all its critical points are non-degenerate and have distinct function values. The *index* of a critical point is the number of negative eigenvalues of H and separates minima, maxima, and saddles.

Although these definitions work well for smooth functions, computing critical points is non-trivial for discrete representations, which lack proper differentiability. Banchoff [Ban70] computes the critical points of a function on a closed, triangulated 2-manifold. The function is defined as the distance to a fixed plane P and assumed to be *general*, i.e., the values at vertices are distinct. In this case, critical points coincide with vertices. To determine the type of a point p, Banchoff considered how the star of p, i.e., the set of simplices containing p, is intersected by a plane through p parallel to P. Edelsbrunner et al. [EH04] determine a point's type and index based on the homology of p's lower link, i.e., the subcomplex induced by the vertices of lower function value of p's star.

Functions of interest to visualizations are often afflicted by noise causing a large number of critical points. *Topological simplification* removes critical points, preferably only those due to noise, and often constructs a similar function with fewer critical points. Edelsbrunner et al. [ELZ02] use *persistent homology* to drive topological simplification. This construct is often introduced starting from a set of points that are turned into a one-parameter filtration of a cell complex via geometric methods, but our discussion will start with its topological treatment. Given a filtration, i.e., a sequence of simplicial complexes where each simplicial complex is a subcomplex of the next, persistent homology notes points in the sequence where the complex's homology changes, reflecting the creation or closing of connected components, tunnels, and voids. Since these events coincide with critical values, critical points responsible for the lifetime of a feature can be paired. Persistence is defined as the "duration" of a feature, and topological simplification removes critical point pairs in the order of lowest persistence. Bauer et al. [BKR14] present a parallel algorithm to compute persistent homology.

Persistent homology in general is surveyed by Edelsbrunner and Harer [EH08]; we will focus on visual representations and their applications. Critical point pairs can be represented as a barcode or a persistence diagram [ELZ02]. A barcode is a set of horizontal lines representing the lifetimes of critical pairs. A persistence diagram is a scatter plot where each critical point pair is drawn as a point using the begin and end time as x, y coordinates. A pair's persistence is thus indicated by the vertical distance to the main diagonal. Rieck et al. [RML12] presented a visual design for persistent homology chains in a radial layout to support visual discrimination between datasets. Rieck and Leitte [RL14] illustrate the geometry of persistent features using a force-directed layout on a graph encoding simplex adjacency. In [RL15], they used persistence diagrams to assess the quality of dimension reduction methods. While there are extensions of persistent homology, e.g. extended persistent homology and persistence modules, to our knowledge none of them have been used for visualization purposes yet, and are not discussed here.

3.1.2. Level Set Methods

A number of topology-based techniques are level set-based. A *level set* is the preimage of a function $f : \Omega \to \mathbb{R}$ for some value v: $f^{-1}(v) = \{p \in \Omega | f(p) = v\}$; it may consist of multiple connected components called *contours*. The *Reeb graph* [Ree46] of a function is the quotient space on $\Omega_{/\sim}$ induced by the equivalence relation $p \sim q$ if p, q belong to the same contour. If the domain Ω is *simply connected*, i.e., every simple closed curve in Ω can be smoothly contracted to a point, the Reeb graph of f is a tree and then called the *contour tree* [BR63]. For this simpler case, there exist multiple efficient algorithms and alternate visual representation.
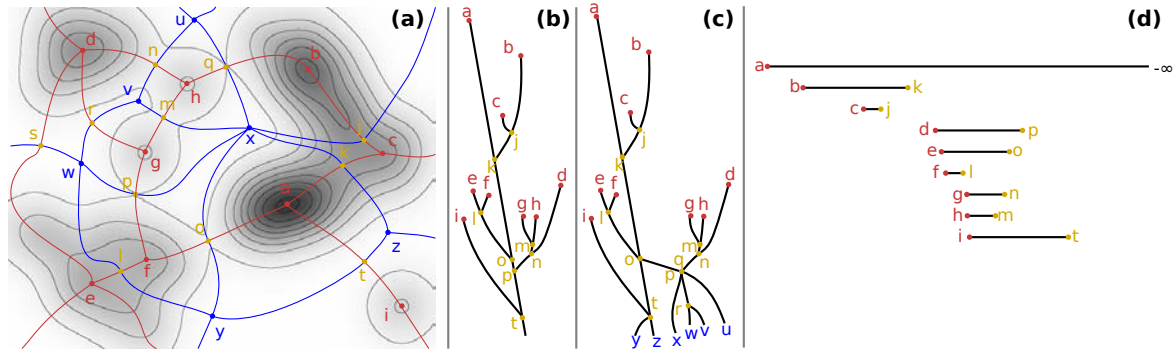
Figure 1: *The image in (a) shows a scalar function and marks contours in black, local maxima in red, local minima in blue, saddles in yellow. Red lines mark the descending cells and blue lines the ascending cells of saddles. The subdivision described by these points and lines is the Morse-Smale complex. Red points and lines plus the saddles form the maximum graph and blue points and lines plus the saddles form the minimum graph. (b) shows the superlevel set merge tree and (c) the contour tree. (d) shows persistent homology for the superlevel set filtration via barcodes. The pairs starting at a red node are in the H_0 homology classes representing the life of connected components.*

Like level sets, sublevel sets $\{p \in \Omega | f(p) \leq v\}$ and superlevel sets $\{p \in \Omega | f(p) \geq v\}$ may consist of multiple connected components. Equivalence among points can be defined similarly: $p \sim q$ if $f(p) = f(q) = v$ and they belong to the same component of the sublevel/superlevel set for v. As long as the domain is connected, the induced quotient space for each equivalence relation is always a tree and is known under many names in the literature: join tree, split tree, level set tree, volume skeleton tree, and barrier tree (for functions on vertices of a graphs). We will refer to them as sublevel/superlevel set *merge trees*. Even though their interpretation varies among domains, their algorithmic treatment and visual representations are mostly interchangeable.

A filtration for persistent homology may be viewed as a sequence of growing sublevel sets of a piecewise constant function. Level set graphs thus relate to persistent homology: graph nodes represent critical points and changing level set homology. But because they only consider connected component relations, critical points where higher-order homology changes are not in the graphs. Some algorithms add these missing critical points back in; following a recommendation by Chiang et al. [CLLR05], we refer to the resulting structures *Reeb topology graph* and *contour topology tree*.

Merge Tree Carr et al. [CSA03] give an efficient algorithm to compute the merge tree for piecewise linear functions on domains of any dimension. They first sort the input mesh vertices based on function value, breaking ties using simulation of simplicity [EM90]. They then initialize one set for each mesh node in a union-find data structure, and for each node v in sorting order, merge the sets of its already processed grid neighbors, adding an edge from each set's lowest node to the current node in the tree. This part runs in $O(m\alpha^{-1}(n))$, where n is the number mesh vertices, m the number or mesh edges, and α^{-1} is the slowly growing inverse Ackermann function. The algorithm is highly similar to the construction of barrier trees for functions on graphs [FHSW02].

Morozov and Weber [MW13] use a special data structure called *skip trees* for the distributed computation of the merge tree. It avoids the communication-heavy parts of the computation by inter-

leaving it with topological simplification. Landge et al. [LPG*14] also compute and store merge trees in a distributed manner, but in addition annotate them so that feature volumes can be reconstructed without needing the original data. They emphasize the need to store boundary extrema for a correct reassembly of merge trees.

Klemelä [Kle04] define the level set tree of a piecewise constant function, approximating a density distribution, as the tree that connects the finite number of superlevel sets according to set inclusion relations. Three visual representation are proposed: a rooted tree drawing, a volume plot, and a barycenter plot. The volume plot modifies the rooted tree drawing by setting the edge thickness proportional to the upper node's associated level set's size. For each dimension of the input space, the barycenter plot assigns each node the barycenter of the associated superlevel set. This allows to judge skewness and kurtosis of the underlying density distribution's modes. Oesterling et al. [OST*10] estimate a density function from a set of input points representing a document collection and then show that function's merge tree as an alternative to clustering.

Oesterling et al. [OHWS13] give an algorithm to construct a landscape profile, i.e. a 1D height function, for a given augmented merge tree. This is the analog of the volume plot for merge trees of functions that are not piecewise constant. Volke et al. [VMH*13] construct a landscape profile for a barrier tree. They then overlay regions in the landscape with histograms showing the performance of different swarm optimization algorithms that operate in the space.

A special subset of merge trees is the *largest contour segmentation*, which is defined as all superlevel set components that contain only one local maximum. It was computed by Manders et al. [MHS*96] for piecewise constant 3D data using region growing and used to automatically mark cells in microscopy images.

Reeb Graph Algorithms for Reeb graph computation and simplification have been surveyed in [BGSF08, BDF*08]. We will only point out fundamental results, and focus on recent progress and visualizations. Shinagawa and Kunii [SK91] give an algorithm to construct a Reeb graph from a set of binary slices. A measure of correspondence between connected components between adjacent

slices is used to define the order of edges that are added to connect these regions until a user-specified number of loops is reached.

Pascucci et al. [PSBM07] give a fast algorithm to compute the Reeb graph from an unordered stream of triangles. The triangles are processed individually, each updating the Reeb graph by adding branches, closing branches, and filling loops. No complexity class is given, but runtime for 3D data was empirically determined close to the theoretical lower bound. Pascucci et al. [PSBM07] proved that the Reeb graph of any piecewise linear function on a simplicial complex is equivalent to the Reeb graph of the function's restriction to the complex's 2-skeleton, i.e. only its points, lines, and triangles. Later work uses this idea to create efficient algorithms for Reeb graph computation; here we only wish to point out a direct deterministic algorithm presented by Parsa [Par13] with time in $O(m \log m)$, m being the size of the input mesh's 2-skeleton, and the algorithm by Doraiswamy and Natarajan [DN13], which assembles the Reeb graph from the contour trees of subvolumes induced by the merge tree. We refer the reader interested in prior work on Reeb graph computation to these references. Dey and Wang [DW12] give an algorithm for the computation of approximate Reeb graphs and their persistence for points sampled from a manifold.

Given the stronger focus on computer graphics and shape description, only a few visual representations and applications have been proposed. Shinagawa and Kunii [SK91] illustrate Reeb graphs using a simple orthogonal graph layout, but no algorithm for computing such a layout is given. Shinagawa et al. [SKK91] use icons to represent nesting in the Reeb graph. Pascucci et al. [PSBM07] give two methods to show the Reeb graph: the first constructs a barycenter skeleton-like representation during computation, the other uses layered graph drawing; both are the predominant display styles.

Regarding applications, Ushizima et al. [UMW*12] reconstruct a Reeb graph from a sliced 3D space and annotate it with amount of thickness to describe material transport and detect pockets. Reeb graphs can be used to describe topological changes with time. E.g., Weber et al. [WBD*11] compute a 4D temperature hypersurface in a time-dependent 3D scalar field resulting from a combustion simulation. They compute the Morse-Smale complex for the fuel consumption rate restricted to this hypersurface, trace its crystals' boundaries with the Reeb graph, and use it as a tracking graph.

Contour Tree Computation Takahashi et al. [TIS*95] construct the contour tree for a piecewise constant function on a 2D structured grid from the 1-skeleton of the function's Morse-Smale complex. De Berg and van Kreveld [dBvK97] compute the contour tree in $O(n \log n)$ time for 2D piecewise linear functions, n being the number of mesh vertices. Carr et al. [CSA03] gave the first $O(n \log n + m\alpha^{-1}(n))$ time algorithm to compute the augmented contour tree for any dimension. They assemble the contour tree from the merge trees for superlevel and sublevel trees in linear time. Chiang et al. [CLLR05] give an algorithm to compute the contour tree for piecewise linear data using monotone paths. After classifying some nodes as component critical, they start paths monotonic in function value from them until they reach a local extremum or an already visited path. In the later case, regions associated with local extrema are merged in an union-find data structure. Only the component-critical points need to be sorted this way and the algorithm runs in $O(n + t \log t)$ time, t giving number of critical points.

Raichel and Seshadhri [RS14] present an algorithm to compute the contour tree in $O(\sum_{c \in C} \log d(c))$ where C is the set of critical points and $d(c)$ denotes the depth of c in the resulting contour tree.

Pascucci and Cole-McLaughlin [PCM03] present an efficient algorithm to compute the contour topology tree in parallel for piecewise trilinear data. They use a divide-and-conquer strategy to give a run time in $O(n + t \log n)$. The method extends to other cell interpolants, provided one can specify an "oracle" which gives the contour tree of a cell. Maadasamy et al. [MDN12] give parallel formulations for the computation of component-critical points and monotone paths. Morozov and Weber [MW14b] present a distributed computation and storage for contour trees. They use a global-local representation internally that reduces communication between nodes during construction and later queries. Carr et al. [CSLA15] present a data-parallel algorithm for computing contour trees for functions quantized in their range.

Contour Tree Simplification Carr et al. [CSvdP10] use different geometric measures to compute the stability of contours. They consider contour length, area, and function value integrated over area for 2D data, contour surface area, enclosed volume and function value integrated over volume for 3D data. They present an $O(n \log n)$ time algorithm to compute a contour hierarchy. Pascucci et al. [PCMS04] present a multiresolution version of contour trees called the *branch decomposition*. They adapt Carr's contour tree algorithm to generate the branch decomposition during computation without additional cost. This representation makes simplification fast and easy to implement. Both Weber et al. [WBP07] and Thomas and Natarajan [TN11] propose a simplification that reduces the depth of the branch hierarchy by moving branches "up the hierarchy" if the difference of saddle function value to the parent branch is small enough. Arge and Revsbæk [AR09] present an I/O-efficient algorithm for contour tree simplification.

Contour Tree Visualization Bajaj et al. [BPS97] present contour trees within their "contour spectrum" interface. They compute and present statistics such as contour length, area, and volume in a histogram-like representation and embed a node-link diagram of the contour tree. No details are given as to how this layout is computed. Both Pascucci and Cole-McLaughlin [PCM03] and Carr et al. [CSvdP10] show the contour tree with a layered graph layout, constraining nodes' *y*-positions to their function value.

Takahashi et al. [TFO09] use an idea from manifold learning to produce drawings resembling contour trees from data given as points in a high-dimensional space plus a function value at each point. They define a geodesic distance between points in the space defined by the *k*-nearest neighbor graphs and the function's values at vertices, then use landmark multidimensional scaling to obtain a projection in 3D. Kraus [Kra10b] uses the simple idea that the area of an isosurface must be the sum of the area of its contours and proposes to visualize contour trees as stacking histograms for each contour tree edge similar to stacked bar charts. A challenge is to avoid edge crossings, for which Kraus uses a simple greedy heuristic. Heine et al. [HSCS11] outline the aesthetic criteria for graph drawings of contour trees and present two algorithms for computing graph drawings subject to a subset of these criteria.

Pascucci et al. [PCMS04] represent a contour tree metaphori-
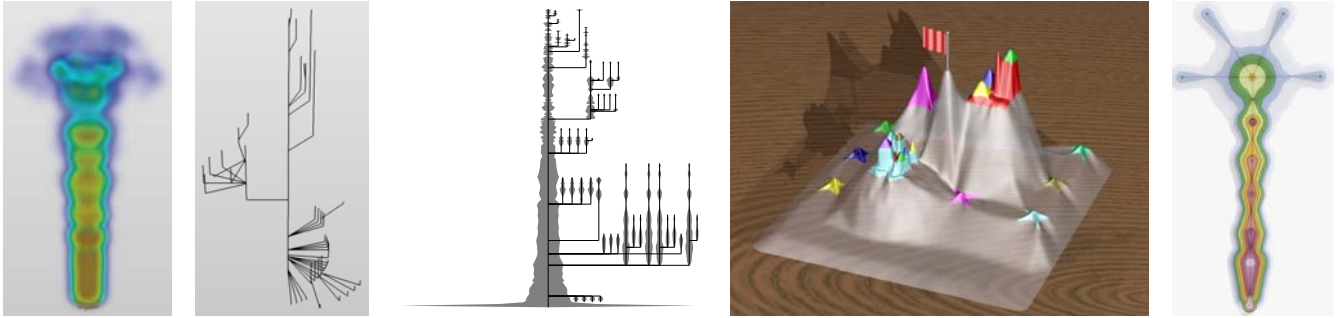
Figure 2: *Different visual representations of the* FUEL *data set – the result of a combustion simulation. Left to right: direct volume rendering; toporrery [PCMS04], graph drawing [HSCS11], and topological landscape [WBP07] of the contour tree (topological landscape image courtesy of Gunther Weber); topological spine of the extremum graph (Image © 2011 IEEE, reproduced, with permission, from [CLB11]).*

cally as a "toporrery" reminiscent of an orrery. The branch hierarchy is laid out in the *x-y*-plane using radial graph drawing and then shifted in *z*-direction based on the node's isovalue. Branches are drawn using an L-shape. An alternate drawing marks the contour tree's critical points in the domain and connects them according to tree edges using straight lines. Weber et al. [WBP12] extend the toporrery design to "topological cacti": they vary line thickness to show geometric properties of contour tree branches.

Weber et al. [WBP07] give a recursive algorithm that constructs a 2D scalar field for a given contour tree and use it to represent the contour tree of a function defined in any dimension. The scalar field is rendered as a terrain and called a "topological landscape". The landscape can be deformed to represent geometric properties of contours. Oesterling et al. [OST*10] use the same core algorithm, but present the resulting 2D scalar field as a color map instead. Harvey and Wang [HW10] recognized the similarity of the problem to tree maps and give a slice-and-dice and a Voronoï-tree-map based construction that also accurately reflects volume contained inside contours. While Weber et al. [WBP07] always chose the global minimum to be represented by the landscape's border, Harvey and Wang [HW10] allow the user to pick any local extremum – causing landscapes to emphasize different structures. The user can pick from a gallery where similar landscape are shown close together.

Fujishiro et al. [FTAT00] suggested to use critical values to guide transfer function design for volume renderings of 3D scalar fields, because at these critical values the topology of isosurfaces changes. Takahashi et al. [TTF04] compute the "volume skeletonization", by which they mean a contour topology tree for a piecewise constant volumetric scalar field, and use it to automatically generate a transfer function for volume rendering. The core idea is to increase opacity near saddle values and vary a spectral color map more strongly in opaque value ranges. Weber et al. [WDC*07] compute the contour tree for 3D scalar fields and identify regions in the volume with tree branches. This allows the user to specify a transfer function for each branch separately; suitable defaults emphasize critical points.

Contour Tree Applications Path seeds by van Kreveld et al. [vKvOB*97] are cell sequences annotated at the contour tree, that can be used to start growing an isosurface for a given isovalue. This enables responsive user interfaces for selecting isosurface.
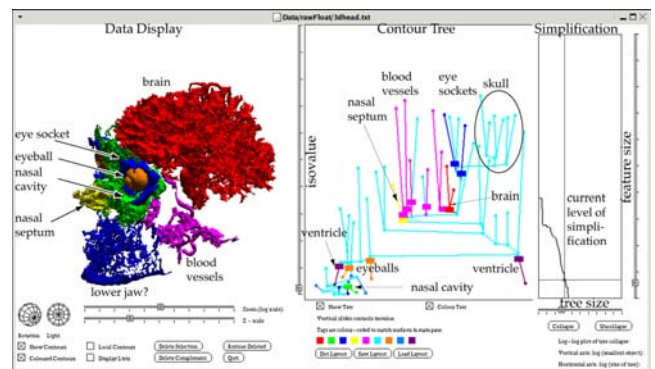
Figure 3: *Flexible isosurface interface for contour selection showing how interactive manipulation of tags in the contour tree (right) leads to a semantic volume segmentation on the left. Image © 2010 Elsevier, reproduced, with permission, from [CSvdP10].*

Carr et al.'s [CSvdP10] "flexible isosurface" user interface allows the user to select, color, and adjust isovalues for contours. They adapt path seeds but use edges rather than 3-cells, giving them a smaller memory footprint. They use their system to extract anatomical parts from volumetric medical scans (cf. Figure 3). Johansson et al. [JMC07] use the flexible isosurface interface to allow the user to specify seed surfaces which are then adjusted locally to give better material boundaries. Bajaj et al. [BGG09] present an application where they use the contour tree of a distance field computed from an isosurface to guide the identification of tunnels and pockets in molecular interaction surfaces. Thomas and Natarajan [TN11] look for similar subtrees within a contour tree to find topologically similar structures, hinting at symmetries in the data. Biedert and Garth [BG15] use the contour tree to automatically segment volumetric data in-situ and represent the result as a set of depth images. These are used in place of the full simulation data for later analysis.

Carr and Snoeyink [CS09] propose to construct so-called widgets for interpolants and construct finite-state automata that represent the possible configurations of level sets with increasing function value. They use the example of the trilinear interpolant and

use their method to prove the correctness of marching cube case tables. Etiene et al. [ENS*12] test the correctness of marching cube algorithm implementations by checking whether they yield triangulations consistent with the contour tree of the trilinear interpolant.

3.1.3. Morse-Smale Complexes

An *integral line* of a smooth function $f : \mathbb{M} \rightarrow \mathbb{R}$ is a maximal curve, where the tangent matches the gradient at each point. Let p be a critical point of index k on f, then the descending k-cell of p is defined by the integral lines that converge on p. Dually, the ascending $(d - k)$-cell of p is defined by integral lines that originate at p. The ascending and descending cells decompose $\mathbb{M}$ into *ascending* and *descending Morse complexes*, respectively. If each non-empty intersection of a descending and an ascending cell is transversal, their connected components define the *Morse-Smale* (MS) complex – a domain partition into regions with equivalent gradient behavior.

Computation There are two foundational theories for computing the Morse-Smale complex on a smooth function's discretization: the piecewise linear Morse theory [Ban70] and the discrete Morse theory [For98]. The former uses Banchoff's characterization of critical points to compute the Morse cells, growing the maximal cells from seeds located at the minima/maxima (region growing approaches), or computing the lines of steepest ascent/descent starting from the saddles (boundary-based approaches). A plethora of works have been presented for computing the Morse complexes from which the MS complex can be derived [DFFIM15].

In [EHZ01] the first algorithm for computing an MS complex on a triangulated 2-manifold has been proposed. The notion of MS complex is adapted to the discrete case in order to guarantee a certain structure to the complex although the preconditions of Morse theory are not respected (i.e., isolated degenerate critical points are present in the data). The notion of *Quasi Morse-Smale (QMS)* complex is introduced and numerical accuracy is achieved via local transformations that preserve the structure of the complex. In the 2D case, a QMS complex is a quadrangulation of the triangle mesh but the 1-cells of the QMS complex are not necessarily those of maximal ascent/descent, as they are in an MS complex. Edelsbrunner et al. [EHNP03] extend the concept and computation of the QMS to tetrahedralized 3-manifolds.

The algorithms described in [BEHP04] and [GNPH07] focus on tracing the lines of steepest ascent/descent more accurately. While in [EHZ01] the steepest slope was evaluated on the edges of the triangle mesh, Bremer et al. [BEHP04] extend the approach allowing separatrix lines to cross triangles. Since tracing separatrix lines across triangles is computationally intensive, a different approach for the 3D case is proposed in [GNPH07] following a region growing schema. The MS complex is computed as collection of vertices, i.e., through vertex labeling. First, minima are found and an ascending 3-cell is grown from each of them. Then, ascending 2-cells are built starting from boundary vertices of 3-cells and finally, ascending 1-cells are built starting from boundary vertices of 2-cells. Descending 3-, 2-, and 1-cells (in this order) are computed inside the ascending 3-cells using the same approach in a symmetric way.

Although easy to implement, all piecewise linear algorithms are generally computationally intensive and not well suited for parallelism. For this reason *Discrete Morse Theory (DMT)* [For98] gathered a lot of attention being an adaptation of Morse theory to the discrete case, defined in a fully combinatorial way. Using DMT a discrete gradient vector field can be computed from sampled data on a cell complex Γ. A vector is defined as a pair of cells (σ, τ) where σ is an k-cell in the immediate boundary of τ (i.e. their dimension differs by 1). A *discrete vector field V* defined on Γ is a collection of pairs such that each cell of Γ is in at most one vector of V. A *V-path* is a sequence $\sigma_1, \tau_1, \sigma_2, \tau_2, ..., \sigma_r, \tau_r$ of k-cells σ_i and $(k+1)$-cells τ_i, $i = 1,..,r$ with $r \geq 1$, such that $(\sigma_i, \tau_i) \in V$, σ_{i+1} is a face of τ_i, and $\sigma_i \neq \sigma_{i+1}$. A V-path with $r > 1$ is *closed* if σ_1 is a face of τ_r different from σ_{r-1}.

A discrete vector field V is a *discrete Forman gradient vector field* (or *Forman gradient*) when there are no closed V-paths in V. A *critical cell* of V of index k is a k-cell γ which does not appear in any pair of V. Following the V-paths starting and having destination in a critical simplex, the Morse cells can be computed efficiently.

Most algorithms concentrate on computing the Forman gradient from the data sampled at the vertices of a cell complex. The algorithm described in [GBHP08] is the first one to introduce a divide-and-conquer approach for computing a Forman gradient on real data. However, many spurious critical simplices are identified during the gradient computation that have to be removed later, thus affecting time performances and topological accuracy.

Shivashankar et al. [SMN12] define a similar approach for piecewise bilinear functions. The algorithm provided is GPU-based and out-of-core, but still introduces artificial critical simplices. In [SN12] the method is extended to piecewise trilinear functions. Saddle-extremum connections are still computed on the GPU, but saddle-saddle connections concurrently on the CPU.

In [RWS11] a dimension-agnostic algorithm is proposed that processes the lower star of each vertex independently. It has been proved that up to the 3D case, the critical cells identified are in one-to-one correspondence with the topological changes in the sublevel sets, i.e. no spurious critical simplices are created. The algorithm has been extended in [FIDFW14] and [WIFDF13] for triangle and tetrahedral meshes, respectively; they provide the first compact representation for a Forman gradient on simplicial complexes.

Even if faster and topologically more accurate, algorithms based on DMT share a problem with methods rooted in piecewise linear Morse theory. In general, none of them converge to the ground truth smooth function when the underlying discrete domain is refined. To address this problem, Gyulassy et al. [GBP12] present a probabilistic algorithm for discrete gradients and deterministic algorithms for 2D and 3D data to compute more accurate manifold geometry.

When working with high-dimensional data, only a subset of the Morse-Smale cells is considered, in particular for visualization purposes. Gerber et al. [GBPW10] approximate the Morse-Smale complex for high-dimensional data by computing the maximal cells of the MS complex on the point cloud directly. Descending Morse cells are computed by connecting points via k-nearest neighbor and by assigning a maximum to each node; ascending Morse cells are computed analogously. The Morse crystals (maximal cells of the MS complex) are created collecting vertices with the same label

pair. Because these approximated Morse crystals can be non-simply connected, Harvey et al. [HRP*12] use the Reeb graph of such crystals to find and close spurious loops.

Correa et al. [CLB11] introduced *topological spines* – a planar visual representation of a *d*-dimensional piecewise linear scalar field, based on its extremum graph. An extremum graph can be computed from the descending or ascending Morse complex. The maximum graph $G = (V, E)$ is the extremum graph computed from the descending Morse complex Γ and representing the adjacency relations of its maximal cells, i.e., V consists of the maximal cells of Γ and vertices are connected if and only if the corresponding descending cells are adjacent in Γ. Dually, the minimum graph can be computed from the ascending Morse complex.

Simplification Simplification of an MS complex is a fundamental step to create effective descriptors of a scalar field. The huge size of the datasets and the presence of noise make reducing the number of critical points crucial. A *k-cancellation* is a simplification operator defined in Morse theory that transforms the ascending and descending Morse complexes into complexes with fewer cells. Let p be a $(k+1)$-cell and q a k-cell, with $k = 0, \ldots, d-1$ of a descending Morse complex. A *k*-cancellation is performed provided that q is incident in p only once. The *k-cancellation*(p, q) removes cells p and q and changes the connectivity of the remaining cells.

Two different approaches for applying the *cancellation* operator exist in the discrete case, depending on the structure used for representing the MS complex. The first approach works on a graph-based representation of the MS complex [EHZ01, BEHP04, ČD11]. Each simplification removes a pair of critical points merging the corresponding Morse cells explicitly (i.e., collapsing the nodes of the graph). This method requires all the MS cells to be computed before starting the simplification algorithm.

In [For98], the *cancellation* operator is described in terms of updates on the Forman gradient V. The *k-cancellation*(q, p) operator deletes a critical k-simplex q and a critical $(k+1)$-simplex p if and only if p and q are connected through exactly one V-path. The effect of a *k-cancellation*(q, p) on V is to reverse the gradient arrows on the V-path between p and q pairing, as a consequence, both p and q. Algorithms developed for a Forman gradient [WGS10, GSW12, FIDFW14] are typically slower since they have to update, for each simplification, all the gradient pairs along the V-path. On the other hand, they exploit the implicit representation the Forman gradient provides, resulting in low storage costs.

The two methods are equivalent when working in 2D but may create different results when working in three or higher dimensions. As described in [GRSW14], the connectivity among the critical cells involved in a 1-*cancellation* between saddles may change without control, thus leading to topologically inconsistent representations. In [IFD15] the first simplification algorithm that solves this problem is presented, based on the operator introduced in [ČD11].

Most of these works considered only the simplification of the MS complexes and not the modification of the original scalar function according to the topological simplification. Bremer et al. [BEHP04] numerically modify the function, defined on a triangulated domain, using Laplacian smoothing after each *cancellation*, in order to agree with the new topology. In [WGS10], the bottleneck of the

smoothing step performed after each *cancellation* in [BEHP04] is solved by constructing a topologically valid function after all the *cancellation* steps, resulting in a faster process. Günther et al. [GJR*14] present a method to smooth a given input scalar function while preserving a user-specified set of local extrema, operating directly on a discrete gradient field representation of the input.

A different take on simplification is based on scale-space approaches, i.e. considering the stability of critical points in a family of functions generated by a smoothing operator. Reininghaus et al. [RKG*11] use a DMT-based approach to compute a measure of persistence that, compared to persistent-homology-based approaches takes each critical point's Morse cell size into account.

Visualization The first complete characterization of the features that can be visualized from an MS complex is provided in [GKK*12]. All the different information that can be extracted from the Morse cells, as well as the decomposition provided by the MS complex, are discussed with graphical examples. Moreover, a tool for the multiresolution representation of MS complexes is described providing the first visualization framework for the interactive investigation of a scalar field based on Morse features. While fundamental when working in two or three dimensions, the above visualization framework is suboptimal for high-dimensional data.

To address this problem, Gerber et al. [GBPW10] combined a topological and a geometric technique for obtaining a new method for the visual exploration of data in high dimensions. The MS complex is used here as a segmentation schema. A regression curve is computed for each cell of the MS decomposition and augmented with local information such as sampling density, standard deviation, and function value. The same problem is faced by Correa et al. [CLB11], where they use a force-directed graph layout to position the vertices. In addition, contour nesting and contour volume are computed and shown as an overlay on the graph layout.

Applications Morse and Morse-Smale complexes have been used in a variety of applications fields, including geographic information systems, biology, and medicine.

Gyulassy et al. [GDN*07] use a topologically simplified Morse-Smale complex of a signed distance field computed from a 3D iso-surface to find the skeleton of a porous material. They can modify the distance field to give the smallest number of critical points, prune "fingers", and straighten arcs of the Morse-Smale complex.

Simplified Morse-Smale complexes computed on real data have been used in [GBC*14]. The MS complex is used as a topological representation of molecular interactions (i.e., covalent and non-covalent bonds) for studying chemical systems through visualization. In [NKWH08], a hierarchy of simplifications on the MS complex is computed and stored to study biomolecular surfaces.

In [GGL*14], a combination of the region-growing algorithm described in [GNPH07] and of the Forman gradient computation described in [RWS11] is defined. The MS complex is used here for the automated segmentation in histopathology. The Forman gradient is computed constrained to an MS segmentation obtained semi-automatically: a domain expert removes false negatives from an initial segmentation with the algorithm from [GNPH07].

Correa and Lindstrom [CL11] use extremum graphs to assess the accuracy of different geometric graphs that reconstruct connectivity from high-dimensional point sets. They study *k*-nearest neighbor graphs, Delaunay triangulations, nearest neighbor graphs, relative neighborhood graphs, Gabriel graphs, diamond graphs, β-skeletons, as well as their own generalizations of the later five. Thomas and Natarajan [TN13] use augmented extremum graphs to detect topologically and, in part, geometrically similar substructures for a user-provided "query" structure. They also use them to generate transfer functions for volume rendering. Maljovec et al. [MWR*16] use linearizations of Morse cells to enable the study of parameter spaces arising in simulations for reactor safety.

One of the most important applications is the interactive exploration of data based on multiresolution models. Such models provide a hierarchy on which on-line queries can extract morphological representations at different resolutions. Multiresolution models have been developed for terrains [EHZ01, BEHP04, DDMV10], volume data [GKK*12] or have been defined dimension-agnostic [ČDI12]. Some of them have also considered to combine the multiresolution representation of the topology with the underlying geometry. In [BEHP04], the Morse cells are retriangulated after each simplification/refinement for describing the given morphological resolution. The *Multiresolution Morse Triangulation (MMT)* [DDMV10] is a first attempt to simplify both geometry and morphology of a scalar field in a combined and consistent manner. However, it is verbose, and mesh simplification through half-edge collapse may generate new critical points. In [IDF14] a simplification hierarchy based on the *gradient-aware edge-contraction* has been proposed which avoids deleting or creating critical simplices.

3.2. Exact Time-Dependent Scalar Fields

Critical Point Tracking Edelsbrunner and Harer [EH04] outline an idea to use Jacobi sets (see Sec. 6) to track critical points of time-dependent scalar fields. They treat the time-dependent function $f(p,t)$ on a *d*-dimensional domain as a time-independent function on a $(d+1)$-dimensional domain and define a second function $g(p,t) := t$; the Jacobi set of these two functions then traces out the critical points' paths. Jacobi sets have been used by Bremer et al. [BBD*07] to track features for 2D time-dependent scalar fields. They propose to simplify Jacobi sets based on the duration that they persist. Reininghaus et al. [RKWH12] track critical points in 2D time-dependent scalar fields on structured grids by transforming each adjacent time slice into a 3D combinatorial vector field in which detection and tracking critical points amount to a path search. Cohen-Steiner et al. [CSEM06] give an algorithm for updating persistent homology of a filtration when the piecewise linear function changes smoothly. They show that smooth changes in function cause smooth changes in the persistence diagram and define vineyards as the tracks of critical point pairs in these diagrams.

Level Set Tracking A number of level set tracking methods have been proposed and are surveyed in [MS09]. Samtaney et al. [SSZC94] track sublevel sets that are grown from minima until they exceed a geometric measure, e.g. volume or homogeneity. Across time, sublevel sets are identified via spatial overlap and a Reeb graph is constructed by removing edges from a weighted

graph until a user-specified number of components remain. The result is shown using layered graph drawing, color-coded to emphasize merges. Kettner et al. [KRS03] present the Safari interface, where for each time step in a time-dependent scalar field a contour tree is computed to give a histogram for the number of connected components over time and isovalue. Using the system, a user can then select interesting isovalues. Szymczak [Szy05] propose a system called "subdomain-aware contour trees". He computes contour trees for adjacent time-steps and annotates the parts within a domain of interest. His system then allows the user to query, e.g., for sets of contours that will split *n* times more often than they will merge. Sohn and Bajaj [SB06] identify contours through a measure that considers both spatial overlap of the interior and exterior of a pair of contours. Thresholding this measure results in a tracking graph that is presented using layered graph drawing techniques.

Bremer et al. [BWT*11] represent large time-dependent 3D scalar fields by computing one merge tree per time step and annotating its branches with statistical measures for further scalar fields. They track features in time using spatial overlap and allow the user to specify an isovalue for which a tracking graph is generated from the immediate representation. The tracking graph is shown as a layered graph drawing. Building on this work, Widanagamaachchi et al. [WCBP12] consider the problem of updating the graph layout of a tracking graph when the user changes the isovalue of interest. Lukasczyk et al. [LMGH15] use kernel density estimates for points in space and time and show the Reeb graph for one isosurface of the resulting function to visualize spatio-temporal patterns with applications in epidemiology and analyzing crime data.

Dynamic Level Set Graphs Edelsbrunner et al. [EHMP04] compute time-dependent contour trees for scalar fields on a simply-connected 2- or 3-sphere. They track critical points via Jacobi sets, then use the result to update the contour tree initialized for the first time step using an involved case analysis. Mascarenhas and Snoeyink [MS05] note difficulties in implementing the algorithm for 2-manifolds and that turning structured into simplicial grids results in many spurious Jacobi sets. A practical approach requires topological simplification. Edelsbrunner et al. [EHM*08] later extend the approach by annotating the time-dependent contour tree with all changes in homology and path seeds for flexible isosurface extraction. They also discuss challenges when extending the method to 4- or 5-manifolds and non-simply connected domains.

Keller and Bertram [KB07] present the hyper-Reeb graph, which describes a Reeb graph changing in time, and an algorithm to depict this structure as an extension of a similar algorithm for time-independent Reeb graphs. Oesterling et al. [OHW*16] give an algorithm to compute the time-varying version of the merge tree for piecewise linear functions in arbitrary dimensions. Noting that the augmented merge tree's structure only changes when the sorting order of adjacent tree nodes changes, they determine a sequence of local updates to the augmented merge tree. They relate changes in the augmented merge tree to changes in the unaugmented merge tree. They present the results using one layer for each time step containing a 1D landscape profile and indicate correspondences as well as events such as bifurcation and joins via visual links. Heine et al. [HSF*06] present a dynamic graph drawing algorithm for sequences of barrier trees, when given a tracking for tree leaves.

3.3. Uncertain Time-Independent Scalar Fields

For multivariate-Gaussian-distributed functions on 2D and 3D structured grids, Mihai and Westermann [MW14a] present a method to compute "confidence regions" and type probabilities for critical points from the derived Hessian fields. A critical point's confidence region is defined as the set of all points where the trace and determinant of the Hessian are within a confidence interval signifying a critical point. They classify each grid point considering covariance with its 8 neighbors in 2D and 26 neighbors in 3D.

Bubenik [Bub15] constructs an "envelope" function from the persistence diagram of a function and uses linear combinations of these envelopes to provide aggregate visualizations of multiple scalar functions and define some statistical measures like deviation.

Günther et al. [GST14] propose a non-local characterization of critical points and their spatial relation for uncertain piecewise linear functions in 2D. They assume that each grid position is assigned a probability distribution function with finite support and construct an upper and a lower bound function. Recognizing a certain nesting relation of sublevel and superlevel sets of realizations with these bounds, they compute a spatial region and level set value interval for critical points. Nesting is also employed to put critical points into a merge-tree-like structure enabling simplification.

Kraus [Kra10a] uses image operators opening and closing to remove noise from volumetric data on structured grids. The operators are changed slightly to preserve local extrema. Contour trees for the modified data sets are assembled into one super contour tree, indicating similarities and differences using color. To visualize an ensemble of scalar fields, Wu and Zhang [WZ13] compute and simplify a contour tree from the mean field and overlay its graph drawing with glyphs indicating contour variance. Zhang et al. [ZAM15] use a Monte Carlo method to query an uncertain 2D terrain for the probability whether two points lie on an edge in the contour tree and what their expected height difference is.

4. State of the Art – Vector Fields

Formally, a (stationary) vector field v on a manifold $\mathbb{M}$ is a map from the manifold itself into its tangent bundle; every point $x \in \mathbb{M}$ is mapped onto an vector in tangent space. An *integral curve* in v through a point x is the (under reasonable assumptions) unique solution to the first ordinary differential equation with v as its right-hand side and initial condition x. Integral curves capture the notion of transport or advection and are the central elements of study in vector field topology. The closely associated flow of a vector field describes how manifold points move under finite-time advection.

Limit sets and invariant sets represent the basis of most topology-based visualization techniques. While the former are sets of limit points of integral curves in positive and negative time, the latter represent subsets of the vector field domain that are mapped to themselves under the induced flow. By far the largest body of work on the topology-based visualization of vector fields is based on the topological model of limit sets and their connections; these are typically extracted and visualized directly. For a more thorough introduction to these concepts, we refer the reader to [GH83].

In the following, we survey topology-based visualization techniques following the typology laid out in Table 1. Due to available
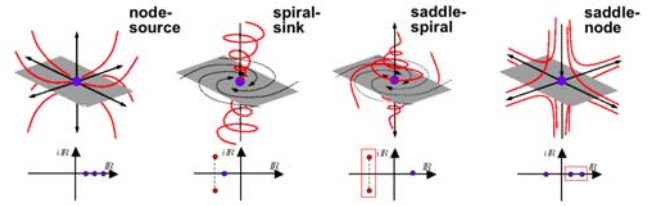

Figure 4: *Classification of critical points in a 3D vector field.*

space, we cannot include a thorough discussion of applications of topology-based vector field visualization; we instead refer the interested reader to the surveys by Laramee et al. [LHZP07, LCJK*09], Pobitzer et al. [PPF*11], and Wang et al. [WWL16] and focus on discussing the most important references per model and explicitly point to recursive references in the cited works.

4.1. Exact Time-Independent Vector Fields

4.1.1. Direct Visualization of Vector Field Topology

Critical Points and Separatrices The works Helman and Hesselink [HH89] and Globus et al. [GLL91] were among the first to extract critical points, i.e. limit sets of dimension zero, from the numerical representation of a flow fields with the aim of visualization. Critical points are easily identified as isolated points where the vector field vanishes (e.g. a velocity is zero); i.e., for a vector field $v : \mathbb{M} \to \mathbb{R}^d$, a point p with $v(p) = \mathbf{0}$ is *critical*. Such points can be classified into several types based on the first-order approximation through the Jacobian matrix ∇v of the vector field in a small neighborhood. In practice, this is achieved by numerical analysis of the eigensystem of the Jacobian matrix. In the case of eigenvalues of mixed sign, a critical point is called a saddle point. Typical types of critical points in a three-dimensional vector field are depicted in Figure 4. As is easy to see, saddle points act as limit sets for integral curves of the form in both positive and negative time.

The specific sets of integral curves whose positive-time limit is a given saddle point is called the saddle's stable or attracting manifold; conversely, curves forming its unstable or repelling manifold reach it in the negative time limit. Often, both sets are uniformly called separatrices, or separation surfaces if they are of dimension two. It can be shown that the quotient of the set of all integral curves with respect to their limit sets forms a partition of the domain into regions of uniform behavior between which there is no transport. In this sense, separatrices act as transport boundaries, and thus the topological model captures the semantics of vector fields exceedingly well. For the purpose of visualization, the decomposition is not typically computed explicitly; rather, depiction of the separatrices is often viewed as sufficient to imply the decomposition, especially in the two-dimensional and surface cases (Figure 5 provides an example). Hauser and Gröller further illustrate this [HG00].

It should be noted in passing that many concepts from scalar field topology correspond to the special case of vector field topology of the scalar's gradient field; for more details, see Section 3.1.3. However, this similarity has not played a major role in topology-based visualization. We will discuss this point further in Section 7.
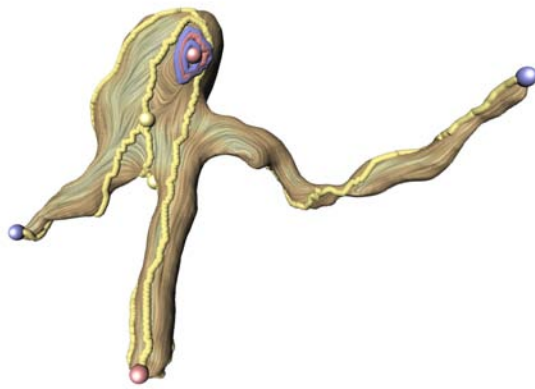
Figure 5: *Direct visualization of critical points and separatrices on a cerebral aneurysm dataset, extracted using the combinatorial approach of Reininghaus and Hotz. Image © 2011 Springer, reproduced, with permission, from [RH11].*

Figure 6: *Indirect visualization of vortex rings (invariant tori) using a Poincaré section [PS07]. Image courtesy of Ronny Peikert.*

Critical point extraction and classification from a tetrahedral discretization with assumed linear interpolation was described by Nielson [NJS*94] and has subsequently been generalized to a variety of computational grid types and interpolants. Mann and Rockwood [MR02] employ Geometric Algebra to identify cells containing critical points (or curves thereof). Scheuermann et al. [SKMR98, SHK*97] extract, classify, and visualize non-linear or higher-order critical points. Corresponding visualization techniques for 3D vector fields are further studied by Weinkauf et al. [WTHS04b]. Bhatia et al. [BGW*14] prove necessary and sufficient conditions for the existence of critical points in a grid cell for a large class of interpolants and from this derive a combinatorial algorithm to identify candidate cells.

Addressing explicitly the computation of separating surfaces, Mahrous et al. [MBS*04] derive a segmentation of a three-dimensional vector field domain by explicitly observing the behavior of integral curves. Separating surfaces then result as segmentation boundaries. Taking a direct approach, Garth et al. [GTS*04a] use the computation of integral surfaces to extract and render separation surfaces. Schneider et al. [SRWS10] improved on this by allowing robust convergence of integral surfaces to critical points. Observing the typically complex geometry of separating surfaces, Theisel et al. [TWHS03] and Weinkauf et al. [WTHS04a] point out *saddle connectors* as a possible solution, reducing separatrix surfaces to curves connecting saddles. England et al. [EKO07] employ a collocation technique to compute (un)stable manifolds from analytical dynamical systems.

Particular attention is given to (two-dimensional) vector fields on curved surfaces by some authors. The vector field topology on such surfaces is intimately connected to fluid flow phenomena such as boundary separation and attachment of a surrounding three-dimensional flow. Following the seminal works of Kenwright et al. [KHL99], who utilize topology extraction to identify separation and attachment lines, Wiebel et al. [WRKS10] visualize surface topology in the context of surrounding flow.
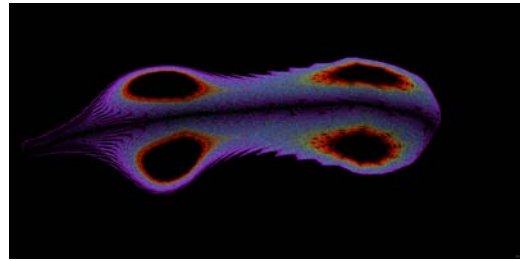
Galilean-Invariant Flow Topology A shortcoming of vector field topology is its lack of *Galilean invariance*. In brief, two observer in relatively moving reference frames will observe different topological skeletons. To address this deficiency, Wiebel et al. [WGS07] proposed the concept of *localized flow* to isolate a specific topological structure independent of observer movement. This idea is substantially extended by Bhatia et al. [BPB14], who show strongly improved results avoiding physically impossible topological structures in some cases. Similar concepts are used by some authors to extend stationary topology-based visualization to the time-varying case, where topological structures are identified in reference frames co-moving with flow particles (cf. Sec. 4.2.3). Bujack et al. [BHJ16] propose a similar yet different approach to address Galilean invariance. By considering every domain point as critical and filtering for persistence (cf. Section 4.1.3), they determine locally dominating frames of reference that are well-suited to visualization.

Combinatorial Techniques In comparison to the numerical approach of many earlier works, purely combinatorial and hybrid techniques have gained ground and promise to forgo inconsistent results and guarantee topological properties such as invariants. A variety of techniques transform continuous vector fields into graph representations from which they then extract topological structures. Reininghaus and Hotz [RH11] leverage *combinatorial vector fields* based on discrete Morse theory for this purpose.

The *edge maps* approach [BJB*11] considers the connectivity of points on the edges of a triangulation for this purpose. Levine et al. [LJB*12] improve on this by turning a continuous vector field into a quantized representation with bounded error. An advantage of combinatorial techniques is the ease of computing a topological segmentation of the vector field domain, which is demonstrated by all these works.

Thus far, combinatorial techniques are limited to two-dimensional stationary fields, and a generalization would appear to be a significant undertaking. A substantial advantage of these methods however is that they can be applied to flows on non-planar surfaces with ease.

Invariant Sets Invariant curves and surfaces with respect to the flow form another class of limit sets that are often of interest in applications, as they isolate specific regions of a vector field's do-

main. Wischgoll et al. [WS01, WS02] describe algorithms to augment classical vector field topology depiction using closed orbits in two- and three-dimensional flows, which they detect by observing re-entry of streamlines in the cells of the discretization grid. The same goal is accomplished by Theisel et al. [TWHS04] using a technique that is independent of the computational grid. Kasten et al. [KRRS14] illustrate the extraction of periodic orbits of saddle type in three-dimensional vector fields.

Peikert et al. [PS09, PS07] visualize invariant sets in vortex rings by using the *Poincaré map*, in which intersections of integral curves with a cutting plane implicitly illustrate invariant tori (cf. Fig. 6); an example is shown in Figure 6. Tricoche et al. [TGS11] and Sanderson et al. [SCT*10] present similar techniques to explicitly extract invariant tori in magnetic fusion simulations.

Chen and co-authors focus on the *Morse decomposition* as a topological model of two-dimensional vector fields [CMLZ08]. The topological structures of a vector field are encoded in the Morse connection graph. From this, they extract Morse sets that capture all invariant sets of the flow, and proceed to classify them using the Conley index [CDS*12]. Szymczak and Zhang [SZ12] provide robust algorithms for Morse decomposition of piecewise-constant vector fields. The general framework is extended by Szymczak and Brunhart-Lupo [SB12], who extract nearly-recurrent components of three-dimensional flows.
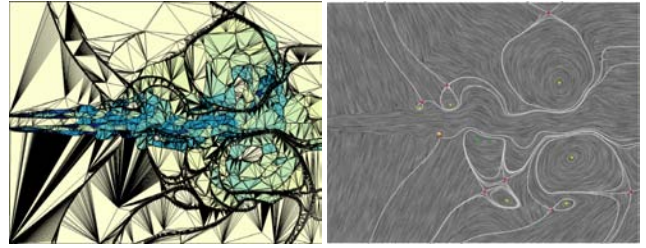
4.1.2. Indirect Visualization

Several methods were presented that do not show the topological skeleton of a vector field directly, but rather use it to derive other visualizations from it. For example, Löffelmann and Gröller [LG98] visualize the flow near topological structures such as critical points and invariant tori of dynamical systems. A similar approach is pursued by Ye et al. [YKP05].

The use of cutting planes (also called section planes by some authors) in conjunction with topology tracking techniques has been shown useful for several specific use cases. Tricoche et al. [TGK*04] introduce so-called *moving section planes* that move through a three-dimensional vector field domain and sample the projected vector field. By tracking topology along the plane movement parameter, they are able to identify vortex cores as trajectories of swirl-type critical points. An extension to the time-varying case is shown by Laramee et al. [LWSH04]. The particular use of section-plane topology to identify flow features is further investigated by Wiebel et al. [WTS09]. They employ moving section planes to identify separation and attachment lines over flow-embedded surfaces.

Instead of canonically embedding the topological skeleton of a three-dimensional flow into its domain, Rössl and Theisel [RT12] proposed more abstract visualization by using multidimensional scaling to obtain an embedding that may be beneficial in interactive visualization of often complex three-dimensional structures.

Reich et al. [RSH*12] convert vector fields into *Morse connection graphs*, from which they isolate topological structures and visualize them using layered graph drawing.

Figure 7: *Topology-preserving approximation of a stream dataset. Left: Coarsened grid. Right: Direct visualization of critical points and separatrices. Image © 2015 Springer, reproduced, with permission, from [KKW*15].*

4.1.3. Simplification and Compression

The *simplification* of topological structures extracted from vector fields has received a considerable amount of attention in the literature. The motivation for this is two-fold. First, both numerical and combinatorial techniques suffer from discretization artifacts that result in erroneous visualization, often in the form of a large number of small-scale structures. Furthermore, the increasing structural complexity of vector fields in applications leads to visualizations that are difficult to understand. In this context, simplification techniques aim to abstract from small-scale behavior, reducing artifacts and providing more comprehensible visualization. A major benefit of topological simplification (as opposed to other filtering techniques that reduce complexity, e.g. smoothing) is that consistency can be explicitly enforced on the level of topological structure, yielding an always consistent (but not necessarily accurate) result.

For two-dimensional vector fields, de Leeuw and van Liere [dLvL00, dLvL99] compare implicit and explicit filtering and collapse critical points and regions of the topological segmentation based on distance and area metrics, but do not enforce consistency. Tricoche et al. [TSH01a, TSH00, TSHC01] cluster nearby linear critical points and replace clusters by higher-order critical points, conserving global consistency. Weinkauf et al. [WTS*05] provide a similar technique for three-dimensional vector fields. More recently, Skraba et al. [SRW*16] describe a framework for the direct cancellation of pairs or groups of critical points in a three-dimensional vector field with guaranteed minimum perturbation.

The approach of Reininghaus et al. [RH11] is based on computing a combinatorial vector field from a discrete one; the corresponding computation can be explicitly controlled to yield a consistently simplified result. Similarly, Morse sets [CDS*12, SZ12] can be computed in hierarchical fashion and thus possess a built-in simplification scheme.

Theisel et al. [TRS03a] further investigate the aspect of compressing a vector field while preserving the topological skeleton. A further approach towards reducing the storage complexity of vector fields while preserving their topological structures is given by Koch et al. [KKW*15] (cf. Figure 7).
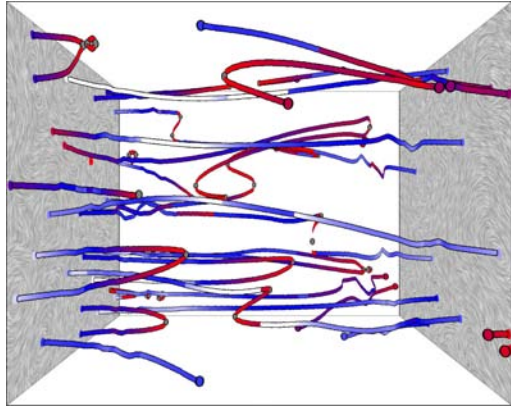
Figure 8: *Tracking graph of a two-dimensional vector field shown using a 2D+time embedding. Colors indicate robustness of critical points and allow the separation of features from noise. Image © 2013 John Wiley and Sons, reproduced, with permission, from [WRS*13].*

4.2. Exact Time-Dependent Vector Fields

The transition from the stationary to the time-dependent case has proven difficult for topology-based methods, and a complete extension of time-invariant topology-based visualization has remained elusive. Largely, corresponding techniques fall into three classes, examined in the following.

4.2.1. Topology Tracking

Parametric topology visualization (or *topology tracking*) interprets time as the parameter in a parametric family of vector fields, and examines the changes in topological structure as the parameter is varied. For some applications, especially those where the vector field varies very slowly compared to the transport processes it describes, this approach is well-founded. A crucial insight underlying most topology tracking approaches is that as the parameter is varied, changes in topology occur only at so-called *bifurcation events* [AS92], where limit sets appear, are annihilated, or change their type. This evolution is often captured in the form of a *tracking graph* that illustrates the movement and bifurcations of critical points and other limit sets by adding time as an additional axis (cf. Figure 8).

For the case of two-dimensional flows, Tricoche et al. [TWSH02] utilize a cell-wise continuation technique to compute the evolution of critical points and their bifurcations over time, assuming linear interpolation between successive time slices of a discrete vector field. They compute and visualize both the trajectories of critical points over time as well as the surfaces traced out by separatrices. Garth et al. [GTS04b] extend this approach to the three-dimensional case. However, as depiction of the (four-dimensional) trajectories is difficult, they propose a two-dimensional graph representation of critical point evolution obtained using a projection approach. To avoid small-scale noise introduced by the (not always suitable) assumption of linear interpolation in time, they filter critical points based on lifetime.

Wischgoll and Scheuermann [WSH01] track the evolution of closed orbits in planar time-dependent flows and detect corresponding bifurcation events. Krauskopf et al. [KOD09] investigate parameter-dependent behavior for general dynamical systems on the example of the Lorentz attractor.

Theisel et al. embed the tracking problem into the *feature flow field* framework [TS03]. By considering time as a spatial dimension along which integral curves propagate with constant velocity, they are able to employ methods for stationary 3D vector fields to both identify critical point trajectories and bifurcation events. A later extension to their work is furthermore suitable to detect closed orbits and global bifurcations [TWHS05]. Weinkauf et al. furthermore provided numerical improvements to the original technique [WTGP11].

Wang et al. [WRS*13] provide a sophisticated framework to investigate *robustness* of critical points that encodes its stability under small perturbations; this allows effective separation of features from noise. Similarly, Skraba et al. develop a simplification algorithm for time-varying critical points based on degree theory [SWCR15].

4.2.2. Lagrangian Coherent Structures

The visualization of *Lagrangian coherent structures* (LCS) is able to elucidate fast dynamics in quickly changing flows. Essentially, LCS capture a dynamic skeleton of time-varying flows by observing the finite-time nature of advection, as opposed to the infinite-time limit sets characterized in vector field topology. However, it should be noted that strictly speaking, LCS do not define a topology (or topological segmentation) in the mathematical sense. Due to the fruitful research addressing LCS, and their roots in dynamical systems theory, we nevertheless view them as a topological model.

Haller [Hal02] first characterized LCS as finite-time attracting or repelling structures via computation of *Finite-Time Lyapunov Exponent* (FTLE) fields. Shadden et al. [SLM05] further illustrated that ridges in these fields may be interpreted as finite-time transport barriers. From a visualization perspective, direct depiction of the FTLE fields may be sufficient to convey the temporal dynamics of a vector field. However, the computation of these fields is very laborious. This problem can be ameliorated using, e.g., GPU computing (e.g., [GLT*09]) for small vector field datasets. To facilitate a more general setting, Sadlo et al. [SP07] and Garth et al. [GGTH07] developed adaptive computation methods. Kasten et al. [KPH*09] and later Kuhn et al. [KRWT12] investigated the effect of varying computational schemes pertaining to the computation of FTLE fields. An extension to studying separation and attachment was given by Garth et al. [GWT*08].

Sadlo and Peikert [SP09] investigate the relationship between LCS and vector field topology in the stationary case, and showed that LCS visualization is in some cases advantageous over direct depiction of topological structures.

A variety of authors have proposed further schemes to investigate the extraction and use of LCS in a general context but independent from visualization; due to the limited space available here, we refer the reader to several recent works [PD10, HSW11, KER*14, MBESar] and recursive references therein for a more complete overview.
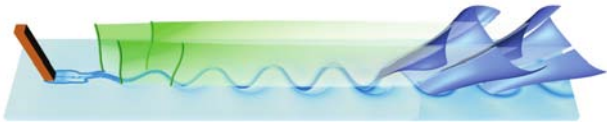
Figure 9: *Streak manifolds from saddle-type trajectories generalize stationary saddle points to time-varying flow. Image © 2013 IEEE, reproduced, with permission, from [ÜSE13].*

4.2.3. Alternate Approaches

Kasten et al. [KHNH11] propose to use moving reference frames, determined from acceleration magnitude, in which it appears sensible to employ notions of vector field topology to visualize time-varying flows. Fuchs et al. [FKS*10] consider the concept of *unsteadiness* to quantify to what extent this approach is meaningful.

Several authors have considered alternative notions of topology that do not or only in part generalize directly from the stationary case. Sadlo and Weiskopf [SW10] replaced stream lines in stationary fields by streak lines in 2D time-varying vector fields. Through this, they are essentially able to capture stable and unstable manifolds of (possibly moving) saddle-type trajectories that assume the role of saddle critical points from the classical case. Most interestingly, their approach can be viewed as a generalization of the stationary case. An extension of their approach to three-dimensional vector fields was given by Üffinger et al. [ÜSE13] (cf. Figure 9).

A commonality between these methods is that they capture specific structures in a vector field that convey the prevalent dynamics and are reminiscent of elements of flow topology such as critical points and separatrices in the stationary case. However, in our definition they are not topological in the mathematical sense; neither the existence of topological invariants nor a notion of topological equivalence and induced domain decomposition have been shown. Nevertheless, we consider the work in this area promising and view this direction of research as fruitful for the topology-based visualization of time-dependent vector fields.

4.3. Uncertainty in Vector Fields

A nascent area of research is the application of topological concepts to the visualization of vector fields under uncertainty. For background and precise terminology in this context, we point to the excellent analysis by Potter et al. [PRJ12]. We include here also techniques aimed at comparison of vector fields on the basis of topological concepts; while not primarily aimed at uncertainty visualization, such techniques can be applied to understand similarities and differences among members of a vector field ensemble.

A quantitative comparison technique (or distance measure) for stationary two-dimensional vector fields based on the similarity of their critical points is given by Lavin et al. [BH99]. Based upon a specific characterization of critical points in two fields, their distance is then derived from the Earth mover's distance between their sets of critical points. Theisel et al. [TRS03b] employ topology tracking (cf. Section 4.2.1) to determine correspondence between critical points in two stationary, 2D vector fields.
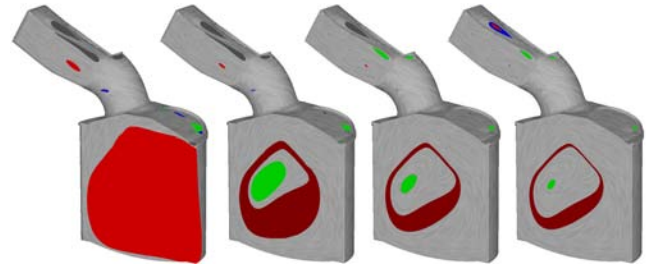
Figure 10: *Morse sets extracted from convex vector fields at increasingly finer resolution capture nearly recurrent flow on surfaces under uncertainty. Image © 2011 John Wiley and Sons, reproduced, with permission, from [Szy11].*

An interpretation of uncertain vector fields as uncorrelated pointwise directional distributions is given by Otto et al. [OGT11b]. It allows to extend computational algorithms from classical vector field topology and straightforward visualization and extraction of critical points using probabilistic integral curves. They show that from this, typical topology-based visualization techniques for stationary "crisp" vector fields can be used. A further extension of this work by the same authors [OGT11a] achieves the same for closed orbits.

Petz et al. [PPH12] adopt a model that includes spatial correlation. Based on this, they investigate probabilistic local features, e.g., critical points in two and three dimension. Their analysis is based on a probabilistic computation of the Poincaré index.

Szymczak et al. [Szy11] introduce the *stable Morse decomposition* of so-called (piecewise-constant and stationary) convex vector fields. Here, the convex hull of multiple vector fields is used to construct a *super-transition graph*, from which Morse sets are obtained that correspond to topological structures (cf. 10). A corresponding visualization is shown in Figure 10. While the approach is intended to investigate the stability of the Morse sets under perturbation (a limited form of uncertainty), it appears useful for more generally uncertain vector fields, i.e. ensembles or stochastic fields with bounded distribution.

Several authors also investigate an extension of the LCS approach (cf. Section 4.2.2) to unsteady vector field ensembles. Schneider et al. [SFRS12] consider replacing FTLE as a basis for LCS with the finite-time variance – more easily extended to include uncertainty – of integral curves in a small neighborhood. Hummel et al. [HOGJ13] also utilize variance measures to distinguish LCS that exist within all members of an ensemble from those that result from variation across an ensemble, thereby providing a more nuanced interpretation of visualization. Directly addressing uncertain vector fields, Guo et al. [GHP*16] derive and visualize a probability density function for LCS obtained using brute-force Monte-Carlo integration.

5. State of the Art – Tensor Fields

The field of tensor visualization often is highly application driven and techniques are designed around special features in the data set. Therefore, few general tensor field visualization techniques exist
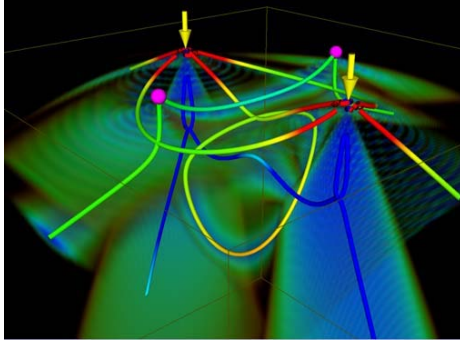
Figure 11: *Triple-degenerate points (magenta) and degenerate lines of a stress tensor field. Yellow arrows indicate points of load. Image © 2005 IEEE, reproduced, with permission, from [ZPP05].*

and many concepts from scalar or vector field topology have not found their way into tensor field visualization, yet. The concept of a tensor of order r, i.e., a multilinear form

$$T : \underbrace{\mathbb{R}^d \times \ldots \times \mathbb{R}^d}_{r} \mapsto \mathbb{R}$$

includes the case of scalars ($r = 0$) and vectors ($r = 1$), which have been discussed before. In this section, we talk about tensors of order two and higher. The majority of literature on tensor field visualization historically focuses on symmetric second-order tensor fields ($r = 2$) either in 2D or in 3D.

Critical points in symmetric second-order tensor fields In a fixed coordinate system, a second-order tensor can be seen as an $d \times d$ matrix. A real, d-dimensional, symmetric matrix M has d (possibly equal) real eigenvalues $\lambda_1 \leq \ldots \leq \lambda_d$ with associated orthogonal eigenvectors $e_1, \ldots, e_d$. A tensor line is a line in a symmetric, second-order tensor field $f : \Omega \mapsto \mathbb{R}^{d \times d}$ that is everywhere tangential to the eigenvector of the i-th eigenvalue [DH94]. At points where at least two eigenvalues are identical, the sorting cannot be performed unambiguously and the tensor line becomes undefined; these are called *degenerate points*.

Looking at two-dimensional tensor fields ($d = 2$), first-order degenerate points can be classified similarly to vector field critical points based on a modification of the Poincaré index, which, due to the directional ambiguity of the lines, is a multiple of $\frac{1}{2}$. The relevant indices for first-order degenerate points are $-\frac{1}{2}$ for a trisector and $\frac{1}{2}$ for a wedge point.

Wedge points have one or two dedicated directions separating a hyperbolic from a parabolic section. Trisector points have three dedicated directions separating three hyperbolic sectors. Both types of degenerate points can be seen as an analogue to saddle points in vector fields, and they form the seed points of a topological skeleton in 2D. Auer and Hotz [AH11] introduced an algorithm to compute a complete topology on 2D manifolds in 3D.

Tracking of degenerate points over time has been first introduced by Tricoche et al. [TSH01b]. The property of merging and splitting critical points can be used for tensor field simplification [TSHC01].

Degenerate lines in 3D tensor fields In 3D symmetric second-order tensor fields, degenerate points can be classified according to the eigenvalues that are equal. If major and medium eigenvalue are equal, the tensor can be described as planar, if medium and minor eigenvalue are equal, it is said to be linear. Zheng et al. [ZP04,ZPP05] point out that planar and linear degenerate points form stable line structures in 3D. Purely isotropic degenerate points are unstable in 3D.

Lagrangian definitions Similar to vector fields, a Lagrangian metaphor may be used to display similar behavior in tensor fields. Tricoche et al. [THBG12] show that LCS ridges on the eigenvector fields mainly correspond to separating surfaces in the tensor field.

Uncertain tensor fields Little work has been done to combine uncertainty with topological features in tensor fields. The only application that falls into this category is the combination of probabilistic tractography in magnetic resonance imaging data with a focus on a topological analysis. Therefore, Schultz et al. [STS07] use the definition of Zheng et al. [ZPP05] on lines tracked with random perturbation together with a clustering technique to extract line-features in MRI data. As it is only based on a line tracking technique, it is not restricted to second order tensor fields. Nevertheless, its applicability may be limited to MRI data.

Higher-order tensor data Even though higher-order tensor glyphs have been studied in more detail, there is no unique definition of topology for higher-order tensors yet. Hlawitschka et al. [HSA*07] defined lines in higher-order tensor fields in 3D and derived a definition for degenerate points as an extension to second-order tensor fields. This leads to a definition of critical points and critical lines, but so far, there is no efficient algorithm for calculating those structures. Schultz [Sch11] proposed a tensor decomposition technique for 2D fields to derive multiple vector fields from tensor fields. Lines of discontinuity in those fields can be seen as a topological skeleton of the field.

Non-symmetric second-order tensor fields Even though the higher-order techniques include the non-symmetric case, special approaches have been defined for non-symmetric second order tensor fields. Zheng and Pang [ZP04] describe the topology of asymmetric tensor fields by introducing the concept of the dual eigenvector to define lines in areas, where the tensors are not symmetric. Lin et al. [LYL*12] derive two graph-based representations of tensor fields called eigenvector and eigenvalue graph. They use the concepts introduce by Zhen and Pang to define the eigenvector graph of a tensor field as a graph with nodes for each area on the eigenvector manifold, which segments the field, and a node for each degenerate point. These nodes are then linked by edges representing their neighborhood relationship in the domain. For the eigenvalue graph, the same concept is followed, but the segmentation is performed by the eigenvalue manifold, segmenting the field into areas where positive or negative scaling, clockwise or counterclockwise rotation, or anisotropic stretching is dominant.

Applications Possible application of tensor field topology is as broad as the variety of data itself and has to be tailored and interpreted according to the meaning of the data. The original papers
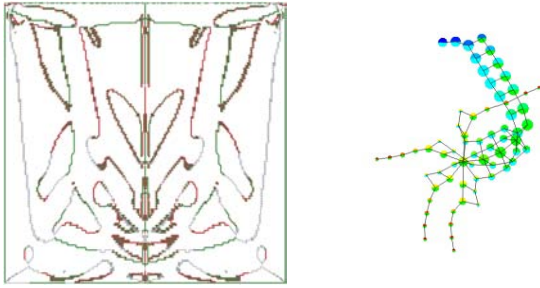
Figure 12: *Left: Jacobi set (black and colored), Pareto maxima (red), and Pareto minima (green) of two scalar fields on a 2D slice from a 3D cylindrical flow simulation. Image © 2013 John Wiley and Sons, reproduced, with permission, from [HHC*13]. Right: graph drawing of a joint contour net for 3 scalar fields . Nodes describe connected regions of similar values (given by color) and edges show region adjacency. Image © 2013 IEEE, reproduced, with permission, from [CD13].*

show hyperstreamlines in tensor fields from mechanical engineering such as earthquake simulations. The single point load and double point load data set are known as reference data sets and are available as material stress and as strain fields. Topological definitions in the terms of segmenting the domain in a variety of behaviors has been done in the study of earthquakes [PLC*11] by interpreting segmentations of the domain.

As topological features may be boundary induced, a direct application of tensor field topology to brain data is challenging due to the brain's complex surface. There, topological features on derived values instead of the tensor data directly show promising results [Sch11, THBG12, HVSW11].

6. State of the Art – Multifields

Edelsbrunner and Harer [EH04] define the *Jacobi set* of k real-valued Morse functions defined on a common d-manifold as the set of critical points of one function restricted to all preimages of the remaining functions. There are multiple equivalent definitions: the Jacobi set can also be defined as the set of all points where the function's gradients are linearly dependent. This definition highlights that when $k > d$ all points become trivially Jacobi, and Jacobi sets are no longer expressive. The authors show that for $k = 2$ generic functions, the Jacobi set is a 1-manifold. In the piecewise linear setting, they present an algorithm for computing Jacobi sets as a set of grid edges, decomposed into simple cycles. Jacobi sets are typically shown by embedding their geometry in the domain.

Edelsbrunner et al. [EHNP04] extent the concept of Jacobi sets to a measure of local or global (averaging over the local measure) similarity of functions. The former equals the volume of the parallelepiped spanned by the function's gradients. In the continuous case, a point is in the Jacobi set if this measure is zero. Nagaraj and Natarajan [NN11] adapt this idea to simplify the Jacobi set of two Morse functions on a common 2-manifold. They replace the two functions by a scalar function giving their local similarity and compute the Reeb graph for this function. For piecewise linear data,

the similarity at vertices is estimated as a weighted average over all incident triangles. They then propose an integer linear program and a greedy heuristic to simplify topology subject to a maximum total change in function.

For two 3D scalar fields, Schneider et al. [SWC*08] propose to compute the two field's contour trees, simplify them, then construct the largest contour segmentations. Using spatial overlap, they compute similarity among contours of different fields and present them as an edge-weighted bipartite graph. The user can interactively select contour pairs and study their relation in the original 3D space. Schneider et al. [SHCS13] extend this approach to multifields. Similarity of contours is now computed using mutual information, the resulting k-partite graph is clustered using the Chinese whispers algorithm, and the result presented in a thumbnail gallery to start the exploration process of the user.

Edelsbrunner et al. [EHP08] defined the Reeb space of k real-valued functions on a common d-manifold as the quotient space of the connected components of f's preimages. They show that for piecewise linear data, if the value $\mathbf{c}$ is not in the range of values of the complex's $k-1$-skeleton, the preimage $f^{-1}(\mathbf{c})$ is either empty or a $(d-k)$ manifold (assuming $k \leq d$). Singh et al. [SMC07] presented a structure called mapper for computing a descriptive simplicial complex for scalar multifields. It starts from a topological covering of the function's image and computes the connected components of their preimage, which amount to a covering of the domain. Each cover becomes a vertex in the resulting simplicial complex and simplices are defined for each set of vertices whose associated covers' intersect. The resulting complex's 1-skeleton is shown using force-directed graph drawing. Carr and Duke [CD13] proposed a similar construction called joint contour nets for scalar multifields. They discretize each function's range into equally-sized intervals and construct a graph from connected components of the finite number of preimages of the discretized function. They give an algorithm to compute joint contour nets for piecewise linear data and present them as node-link diagrams using force-directed graph drawing. Nodes are colored to hint at the original functions' values. Joint contour nets are used by Duke et al. [DCK*12] to study nuclear scission processes from an input describing density fields. Although the data is time-dependent, they process each time step separately and detect structural changes in the joint contour nets visually. Chattopadhyay et al. [CCDG14] propose Jacobi structures – the projection of the Jacobi set to the Reeb space of a multifield – which is more expressive than pure Jacobi sets. They compute an approximation using joint contour nets and it is used in recent work [CCD*15] to define a scaling-invariant topological simplification scheme for multifields on domains with simple topology.

Huettenberger et al. [HHC*13] use the concept of dominance relation and Pareto optimality to visualize k scalar-valued fields on a common domain. Let the dominance relation be defined as: $(u_1, \ldots, u_k) \succeq (v_1, \ldots, u_k)$ if and only if $\bigwedge_{1 \leq i \leq k} u_i \geq v_i$. This partial ordering replaces the order relation over the real numbers in the single-scalar-field case. The authors are then able to classify each point p in the domain based on the existence of dominated and dominating points within an ε-neighborhood of p. The possible types are locally Pareto minimal, locally Pareto maximal, locally Pareto optimal, and regular; these extend the notion of local

extrema to multifields but are unable to provide a definition for a multifield saddle. Pareto sets are the union of all non-regular points. The authors gave an algorithm to compute Pareto sets for piecewise linear functions. Huettenberger and Garth [HG15] showed that Pareto sets are a subset of Jacobi sets. Recognizing this relation, Huettenberger et al. [HHG14] used a strategy similar to Nagaraj and Natarajan [NN11] to simplify Pareto sets and remove noise. The results were used by Huettenberger et al. [HFEG15] to study the quality of car manufacturing processes. Furthermore, Huettenberger et al. [HHG16] showed that a directed version of joint contour nets can approximate Pareto sets, hinting at a further relation of these structures.

7. Discussion & Conclusion

In conclusion, we present some observations and relations among topological structures for different data types as well as pressing open problems arising from our literature review.

Empty Cells in our Typology Some cells in Table 1 are empty. There are currently no topological structures defined for the corresponding classes of input data. We attribute this to a combination of both the difficulty of defining such models and the lack of demand from users of visualization, in turn caused by the increased computational cost associated with producing data of the necessary type. In the following, we will discuss links between some of the cells of our typology in order to shed light on possible translational research that could fill them.

Scalar and Vector Fields Morse-Smale complexes for scalar fields and classical vector field topology are linked by gradient computation that turns a scalar field into an irrotational vector field. While this link could be interpreted to indicate that vector field topology is more general than scalar field topology, we would argue that this is not the case. Computational approaches to methods employing gradients assume the input to be a finite-sized approximation of a smooth function on a manifold where the output would converge to the ground truth in the limit with increasing resolution. Level set methods, such as the merge tree or Reeb graphs, can be defined for any function on a topological space and can work naturally with discrete spaces, as evidenced by barrier trees and other methods to study combinatorial optimization processes (cf. Section 3.1.2). Also, if vector field topology were the generalization of scalar field topology, which topological structure for vector fields would correspond to the Reeb graph? Furthermore, the link may exist in theory, but is not used much in practice. Discrete representations for scalar fields are typically piecewise linear (or multilinear), thus their gradients are technically not continuous. Algorithms for scalar fields often try to work around this deficiency. Discretizations of vector fields, on the other hand, are continuous and therefore "smoother by one degree". This discrepancy prohibits interchanging algorithms for the two classes directly.

Loosening the ties of level set methods with smooth Morse functions can lead to simpler and more general algorithms, possibly at the expense of loosing the connection to critical points. Such a shift in perspective can open new avenues for other problem settings. For instance, moving from gradient-based to ordering-relation-based

definition of critical points allowed a thinking outside the box and gave rise to Pareto sets for multifields, which replace order by partial order relations (cf. Section 6).

We also note that via techniques like finite-time Lyapunov exponents and Galilean-invariant vector field topology, vector fields are turned into scalar fields. Although Lagrangian coherent structures are typically computed using geometric ridges, in the scalar setting ridges have a history of approximating the saddle manifolds of Morse-Smale complexes. It would appear useful to further study this connection in future work.

Tensor Fields Event though tensors of different order have been used in scientific visualization, symmetric second-order tensors are prevalent. Techniques based on line integration have been transfered to those tensor fields, but not others. Definitions for the topology of higher-order tensor fields exist, but are tied to concrete applications and do not yet provide a widely-accepted framework. Even though some concepts are shared, a direct link of tensor field topology with either scalar, vector, or multifields similar to the gradient construction that links scalar and vector field topology are not yet known. Establishing such links, e.g. by studying the topology of the Hessian of a scalar field, could advance translational research.

In general, the visualization of tensor field topology has not found its way into many application domains. This may be due to the lack of a proper interpretation for the components of the topological skeleton. Even though the structures can be interpreted in various ways, we identify the application-specific interpretation of tensor field topology as an area for future research.

Multifields We would like to highlight Jacobi sets, which can be cleverly employed for critical point tracking by reducing a time-dependent problem in d-dimensions to a time-independent multifield problem in $d+1$ dimensions. It is interesting to see whether the idea underlying critical point tracking via Jacobi sets can be used to give accurate and fast algorithms for other topological features, e.g., dynamic Morse-Smale complexes or tracking of vector field topology. Treating time as just an additional spatial dimension (e.g., in isosurface tracking), or using computation-heavy similarity estimation & matching for feature identification and tracking, appear inelegant compared to dynamic level set graphs.

A deeper understanding of the relations among topological models, similar to work linking Pareto sets, Jacobi sets, and directed joint contour nets, can help translate research results between related structures. Further reductionism appears possible. Since we define multifields slightly broader than, e.g., parameter ensembles or samples from a distribution of functions, any method that works for multifields is applicable (although not necessarily optimal) to the other cases as well, but not vice versa. Prioritizing research for multifields could indirectly benefit the other cases as well.

Multifields are a rather new addition to the family of topology-based visualization. There are currently not many applications, but we anticipate this situation to improve, as soon as the interpretation of the topological models for real-world problems are clearer.

Uncertainty From our literature review, original approaches appear necessary for one of the current major developments in

topology-based visualization: the incorporation of uncertainty. Naturally initial work has focused on known structures and derived fields (e.g. variance-annotated contour trees, or range-based merge trees for an uncertain function) or combines existing tools such as critical point definition and statistics. Instead we could shift our attention from the points of the domain and their relation to whole functions and their relation regarding the probability function.

Topology-Based Interaction An area neglected by ongoing research is the use of topological abstractions to build intelligent user interfaces for visualization and analytics. In this regard, the examples of topology-controlled volume rendering and the recent work of Weber et al. on combustion visualization must be considered inspiring. Topology-based visualization techniques, having solid mathematical foundations and built-in mechanisms for abstraction and simplification, have the potential to shine and stand on equal footing with techniques from, e.g., the domain of machine learning. We anticipate the interplay between topology-based visualization and visual analytics to deepen.

Topology-Based In Situ Visualization A further class of problems that appears deserving of additional attention from researchers is the utility of topology-based methods in *in-situ* visualization. It would appear that topology-based techniques could play a major role in addressing some of the most pressing issues such as automated data selection for storage, meaningful reduction of data and structural complexity, and providing robust feature definitions for visualization and statistical analysis. As a crucial precondition, parallel computation of topology needs additional attention.

To conclude, while topology-based methods possess an extensive history in visualization, it appears there are still sufficient relevant yet unsolved problems for the current and next generation of visualization researchers.

Acknowledgments

References

[AH11] AUER C., HOTZ I.: Complete tensor field topology on 2D triangulated manifolds embedded in 3D. *Computer Graphics Forum 30*, 3 (2011), 831–840. doi:10.1111/j.1467-8659.2011.01932.x. 15

[AR09] ARGE L., REVSBÆK M.: I/O-efficient contour tree simplification. In *Proceedingds of Algorithms and Computation: 20th International Symposium (ISAAC 2009)*, Dong Y., Du D.-Z., Ibarra O., (Eds.). Springer, 2009, pp. 1155–1165. doi:10.1007/978-3-642-10631-6_116. 5

[AS92] ABRAHAM R., SHAW C.: *Dynamics–the Geometry of Behavior: Global behavior (2nd edition)*. Addison-Wesley, 1992. 13

[Ban70] BANCHOFF T. F.: Critical points and curvature for embedded polyhedral surfaces. *The American Mathematical Monthly 77*, 5 (1970), 475–485. doi:10.2307/2317380. 3, 7

[BBD*07] BREMER P.-T., BRINGA E. M., DUCHAINEAU M. A., GYULASSY A. G., LANEY D., MASCARENHAS A., PASCUCCI V.: Topological feature extraction and tracking. *Journal of Physics: Conference Series 78*, 1 (2007). doi:10.1088/1742-6596/78/1/012007. 9

[BDF*08] BIASOTTI S., DE FLORIANI L., FALCIDIENO B., FROSINI P., GIORGI D., LANDI C., PAPALEO L., SPAGNUOLO M.: Describing shapes by geometrical-topological properties of real functions. *ACM Computing Surveys 40*, 4 (2008). doi:10.1145/1391729.1391731. 1, 4

[BEHP04] BREMER P.-T., EDELSBRUNNER H., HAMANN B., PASCUCCI V.: A topological hierarchy for functions on triangulated surfaces. *IEEE Trans. Vis. Comput. Graph. 10*, 4 (2004), 385–396. doi:10.1109/TVCG.2004.3. 7, 8, 9

[BG15] BIEDERT T., GARTH C.: Contour tree depth images for large data visualization. In *Eurographics Symposium on Parallel Graphics and Visualization* (2015), Dachsbacher C., Navratil P., (Eds.), Eurographics Association, pp. 077–086. doi:10.2312/pgv.20151158. 6

[BGG09] BAJAJ C., GILLETTE A., GOSWAMI S.: Topology based selection and curation of level sets. In Hege et al. [HPS09], pp. 45–58. doi:10.1007/978-3-540-88606-8_4. 6

[BGSF08] BIASOTTI S., GIORGI D., SPAGNUOLO M., FALCIDIENO B.: Reeb graphs for shape analysis and applications. *Theor. Comput. Sci. 392*, 1-3 (2008), 5–22. doi:10.1016/j.tcs.2007.10.018. 1, 4

[BGW*14] BHATIA H., GYULASSY A., WANG H., BREMER P.-T., PASCUCCI V.: Robust detection of singularities in vector fields. In Bremer et al. [BHPP14], pp. 3–18. doi:10.1007/978-3-319-04099-8_1. 11

[BH99] BATRA R., HESSELINK L.: Feature comparisons of 3-D vector fields using earth mover's distance. In *IEEE Visualization* (1999), pp. 105–114. doi:10.1109/VISUAL.1999.809874. 14

[BHJ16] BUJACK R., HLAWITSCHKA M., JOY K. I.: Topology-inspired Galilean invariant vector field analysis. In *Proceedings of the IEEE Pacific Visualization Symposium* (2016), PacificVis, pp. 72–79. doi:10.1109/PACIFICVIS.2016.7465253. 11

[BHPP14] BREMER P.-T., HOTZ I., PASCUCCI V., PEIKERT R. (Eds.): *Topological Methods in Data Analysis and Visualization III*. Mathematics and Visualization. Springer International Publishing, 2014. 18, 20, 21, 22

[BJB*11] BHATIA H., JADHAV S., BREMER P.-T., CHEN G., LEVINE J., NONATO L., PASCUCCI V.: Edge maps: Representing flow with bounded error. In *Visualization Symposium (PacificVis), 2011 IEEE Pacific* (2011), pp. 75–82. doi:10.1109/PACIFICVIS.2011.5742375. 11

[BKR14] BAUER U., KERBER M., REININGHAUS J.: Clear and compress: Computing persistent homology in chunks. In Bremer et al. [BHPP14], pp. 103–117. doi:10.1007/978-3-319-04099-8_7. 3

[BPB14] BHATIA H., PASCUCCI V., BREMER P.: The natural Helmholtz-Hodge decomposition for open-boundary flow analysis. *IEEE Trans. Vis. Comput. Graph. 20*, 11 (2014), 1566–1578. doi:10.1109/TVCG.2014.2312012. 11

[BPS97] BAJAJ C. L., PASCUCCI V., SCHIKORE D. R.: The contour spectrum. In *Proceedings of IEEE Visualization '97* (1997), pp. 167–172. doi:10.1109/VISUAL.1997.663875. 5

[BR63] BOYELL R. L., RUSTON H.: Hybrid techniques for real-time radar simulation. In *Proceedings of the Fall Joint Computer Conference* (1963), AFIPS '63 (Fall), ACM, pp. 445–458. doi:10.1145/1463822.1463869. 3

[Bub15] BUBENIK P.: Statistical topological data analysis using persistence landscapes. *Journal of Machine Learning Research 16*, 1 (2015), 77–102. 10

[BWT*11] BREMER P.-T., WEBER G., TIERNY J., PASCUCCI V., DAY M., BELL J.: Interactive exploration and analysis of large-scale simulations using topology-based data segmentation. *IEEE Trans. Vis. Comput. Graph. 17*, 9 (2011), 1307–1324. doi:10.1109/TVCG.2010.253. 9

[CCD*15] CHATTOPADHYAY A., CARR H., DUKE D., GENG Z., SAEKI O.: Multivariate topology simplification. *ArXiv e-prints* (2015). arXiv:1509.04465. 16

[CCDG14] CHATTOPADHYAY A., CARR H., DUKE D., GENG Z.: Extracting Jacobi structures in Reeb spaces. In *EuroVis - Short Papers* (2014), Elmqvist N., Hlawitschka M., Kennedy J., (Eds.), The Eurographics Association. doi:10.2312/eurovisshort.20141156. 16

[ČD11] ČOMIĆ L., DE FLORIANI L.: Dimension-independent simplification and refinement of Morse complexes. *Graphical Models 73*, 5 (2011), 261–285. doi:10.1016/j.gmod.2011.05.001. 8

[CD13] CARR H., DUKE D.: Joint contour nets: Computation and properties. In *IEEE Pacific Visualization Symposium (PacificVis)* (2013), pp. 161–168. doi:10.1109/PacificVis.2013.6596141. 16

[ČDI12] ČOMIĆ L., DE FLORIANI L., IURICICH F.: Dimension-independent multi-resolution Morse complexes. *Computers & Graphics 36*, 5 (2012), 541–547. doi:10.1016/j.cag.2012.03.010. 9

[CDS*12] CHEN G., DENG Q., SZYMCZAK A., LARAMEE R., ZHANG E.: Morse set classification and hierarchical refinement using Conley index. *IEEE Trans. Vis. Comput. Graph. 18*, 5 (2012), 767–782. doi:10.1109/TVCG.2011.107. 12

[CL11] CORREA C., LINDSTROM P.: Towards robust topology of sparsely sampled data. *IEEE Trans. Vis. Comput. Graph. 17*, 12 (2011), 1852–1861. doi:10.1109/TVCG.2011.245. 9

[CLB11] CORREA C., LINDSTROM P., BREMER P.-T.: Topological spines: A structure-preserving visual representation of scalar fields. *IEEE Trans. Vis. Comput. Graph. 17*, 12 (2011), 1842–1851. doi:10.1109/TVCG.2011.244. 6, 8

[CLLR05] CHIANG Y.-J., LENZ T., LU X., ROTE G.: Simple and optimal output-sensitive construction of contour trees using monotone paths. *Computational Geometry 30*, 2 (2005), 165–195. Special Issue on the 19th European Workshop on Computational Geometry. doi:10.1016/j.comgeo.2004.05.002. 4, 5

[CMLZ08] CHEN G., MISCHAIKOW K., LARAMEE R. S., ZHANG E.: Efficient Morse decompositions of vector fields. *IEEE Trans. Vis. Comput. Graph. 14*, 4 (2008), 848–862. doi:10.1109/TVCG.2008.33. 12

[CS09] CARR H., SNOEYINK J.: Representing interpolant topology for contour tree computation. In Hege et al. [HPS09], pp. 59–73. doi:10.1007/978-3-540-88606-8_5. 6

[CSA03] CARR H., SNOEYINK J., AXEN U.: Computing contour trees in all dimensions. *Computational Geometry 24*, 2 (2003), 75–94. Special Issue on the Fourth CGC Workshop on Computational Geometry. doi:10.1016/S0925-7721(02)00093-7. 4, 5

[CSEM06] COHEN-STEINER D., EDELSBRUNNER H., MOROZOV D.: Vines and vineyards by updating persistence in linear time. *Proceedings of the twenty-second annual symposium on Computational geometry - SCG '06* (2006), 119–126. doi:10.1145/1137856.1137877. 9

[CSLA15] CARR H., SEWELL C. M., LO L.-T., AHRENS J. P.: *Hybrid Data-Parallel Contour Tree Computation*. Tech. rep., Los Alamos National Laboratory (LANL), 2015. 5

[CSvdP10] CARR H., SNOEYINK J., VAN DE PANNE M.: Flexible isosurfaces: Simplifying and displaying scalar topology using the contour tree. *Computational Geometry 43*, 1 (2010), 42–58. Special Issue on the 14th Annual Fall Workshop. doi:10.1016/j.comgeo.2006.05.009. 5, 6

[dBvK97] DE BERG M., VAN KREVELD M.: Trekking in the alps without freezing or getting tired. *Algorithmica 18*, 3 (1997), 306–323. doi:10.1007/PL00009159. 5

[DCK*12] DUKE D., CARR H., KNOLL A., SCHUNCK N., NAM H. A., STASZCZAK A.: Visualizing nuclear scission through a multifield extension of topological analysis. *IEEE Trans. Vis. Comput. Graph. 18*, 12 (2012), 2033–2040. doi:10.1109/TVCG.2012.287. 16

[DDMV10] DANOVARO E., DE FLORIANI L., MAGILLO P., VITALI M.: Multiresolution Morse triangulations. In *Symposium on Solid and Physical Modeling* (2010), Elber G., Fischer A., Keyser J., Kim M.-S., (Eds.), ACM, pp. 183–188. doi:10.1145/1839778.1839806. 9

[DFFIM15] DE FLORIANI L., FUGACCI U., IURICICH F., MAGILLO P.: Morse complexes for shape segmentation and homological analysis: discrete models and algorithms. *Computer Graphics Forum 34*, 2 (2015), 761–785. doi:10.1111/cgf.12596. 1, 7

[DH94] DELMARCELLE T., HESSELINK L.: The topology of symmetric, second-order tensor fields. In *Proceedings of the IEEE Conference on Visualization '94* (1994), VIS '94, pp. 140–147. 15

[DHKS04] DEUSSEN O., HANSEN C. D., KEIM D. A., SAUPE D. (Eds.):. *VisSym 2004, Symposium on Visualization* (2004), Eurographics Association. 20, 25

[dLvL99] DE LEEUW W. C., VAN LIERE R.: Collapsing flow topology using area metrics. In *IEEE Visualization* (1999), pp. 349–354. doi:10.1109/VISUAL.1999.809907. 12

[dLvL00] DE LEEUW W. C., VAN LIERE R.: Multi-level topology for flow visualization. *Computers & Graphics 24*, 3 (2000), 325–331. doi:10.1016/S0097-8493(00)00028-5. 12

[DN13] DORAISWAMY H., NATARAJAN V.: Computing Reeb graphs as a union of contour trees. *IEEE Trans. Vis. Comput. Graph. 19*, 2 (2013), 249–262. doi:10.1109/TVCG.2012.115. 5

[DW12] DEY T. K., WANG Y.: Reeb graphs: Approximation and persistence. *Discrete & Computational Geometry 49*, 1 (2012), 46–73. doi:10.1007/s00454-012-9463-z. 5

[EH04] EDELSBRUNNER H., HARER J.: Jacobi sets. In *Foundations of Computational Mathematics*, Cucker F., DeVore R., Olver P., Süli E., (Eds.). Cambridge University Press, 2004, pp. 37–57. doi:10.1017/CBO9781139106962.003. 3, 9, 16

[EH08] EDELSBRUNNER H., HARER J.: Persistent homology–a survey. *Contemporary Mathematics 453* (2008), 257–282. doi:10.1090/conm/453/08802. 3

[EHM*08] EDELSBRUNNER H., HARER J., MASCARENHAS A., PASCUCCI V., SNOEYINK J.: Time-varying Reeb graphs for continuous space-time data. *Computational Geometry 41*, 3 (2008), 149–166. doi:10.1016/j.comgeo.2007.11.001. 9

[EHMP04] EDELSBRUNNER H., HARER J., MASCARENHAS A., PASCUCCI V.: Time-varying Reeb graphs for continuous space-time data. In *Proceedings of the Twentieth Annual Symposium on Computational Geometry* (2004), SCG '04, ACM, pp. 366–372. doi:10.1145/997817.997872. 9

[EHNP03] EDELSBRUNNER H., HARER J., NATARAJAN V., PASCUCCI V.: Morse-Smale complexes for piecewise linear 3-manifolds. In *Proceedings of the Nineteenth Annual Symposium on Computational Geometry* (2003), SCG '03, ACM, pp. 361–370. doi:10.1145/777792.777846. 7

[EHNP04] EDELSBRUNNER H., HARER J., NATARAJAN V., PASCUCCI V.: Local and global comparison of continuous functions. In *Proceedings of IEEE Visualization '04* (2004), pp. 275–280. doi:10.1109/VISUAL.2004.68. 16

[EHP08] EDELSBRUNNER H., HARER J., PATEL A. K.: Reeb spaces of piecewise linear mappings. In *Proceedings of the Twenty-fourth Annual Symposium on Computational Geometry* (2008), SCG '08, ACM, pp. 242–250. doi:10.1145/1377676.1377720. 16

[EHZ01] EDELSBRUNNER H., HARER J., ZOMORODIAN A.: Hierarchical Morse complexes for piecewise linear 2-manifolds. In *Proceedings of the Seventeenth Annual Symposium on Computational Geometry* (2001), SCG '01, ACM, pp. 70–79. doi:10.1145/378583.378626. 7, 8, 9

[EKO07] ENGLAND J. P., KRAUSKOPF B., OSINGA H. M.: Computing two-dimensional global invariant manifolds in slow-fast systems. *Bifurcation and Chaos, International Journal of 17*, 3 (2007), 805–822. doi:10.1142/S0218127407017562. 11

[ELZ02] EDELSBRUNNER H., LETSCHER D., ZOMORODIAN A.: Topological persistence and simplification. *Discrete & Computational Geometry 28*, 4 (2002), 511–533. doi:10.1007/s00454-002-2885-2. 3

[EM90] EDELSBRUNNER H., MÜCKE E. P.: Simulation of simplicity: A technique to cope with degenerate cases in geometric algorithms. *ACM Transactions on Graphics 9*, 1 (1990), 66–104. doi:10.1145/77635.77639. 4

[ENS*12] ETIENE T., NONATO G., SCHEIDEGGER C., TIERNY J., PETERS T., PASCUCCI V., KIRBY R., SILVA C.: Topology verification for isosurface extraction. *IEEE Trans. Vis. Comput. Graph. 18*, 6 (2012), 952–965. doi:10.1109/TVCG.2011.109. 7

[FH09] FUCHS R., HAUSER H.: Visualization of multi-variate scientific data. *Computer Graphics Forum 28*, 6 (2009), 1670–1690. doi:10.1111/j.1467-8659.2009.01429.x. 1

[FHSW02] FLAMM C., HOFACKER I. L., STADLER P. F., WOLFINGER M. T.: Barrier trees of degenerate landscapes. *International journal of research in physical chemistry and chemical physics 216*, 2 (2002), 155–. doi:10.1524/zpch.2002.216.2.155. 4

[FIDFW14] FELLEGARA R., IURICICH F., DE FLORIANI L., WEISS K.: Efficient computation and simplification of discrete Morse decompositions on triangulated terrains. In *Proceedings of the 22nd ACM SIGSPATIAL International Conference on Advances in Geographic Information Systems* (2014), SIGSPATIAL '14, pp. 223–232. doi:10.1145/2666310.2666412. 7, 8

[FKS*10] FUCHS R., KEMMLER J., SCHINDLER B., WASER J., SADLO F., HAUSER H., PEIKERT R.: Toward a Lagrangian vector field topology. *Comput. Graph. Forum 29*, 3 (2010), 1163–1172. doi:10.1111/j.1467-8659.2009.01686.x. 14

[For98] FORMAN R.: Morse theory for cell complexes. *Advances in mathematics 134*, 1 (1998), 90–145. doi:10.1006/aima.1997.1650. 7, 8

[FTAT00] FUJISHIRO I., TAKESHIMA Y., AZUMA T., TAKAHASHI S.: Volume data mining using 3D field topology analysis. *Computer Graphics and Applications, IEEE 20*, 5 (2000), 46–51. doi:10.1109/38.865879. 6

[GBC*14] GÜNTHER D., BOTO R. A., CONTRERAS-GARCIA J., PIQUEMAL J., TIERNY J.: Characterizing molecular interactions in chemical systems. *IEEE Trans. Vis. Comput. Graph. 20*, 12 (2014), 2476–2485. doi:10.1109/TVCG.2014.2346403. 8

[GBHP08] GUYLASSY A., BREMER P.-T., HAMANN B., PASCUCCI V.: A practical approach to Morse-Smale complex computation: Scalability and generality. *IEEE Trans. Vis. Comput. Graph. 14*, 6 (2008), 1619–1626. doi:10.1109/TVCG.2008.110. 7

[GBP12] GYULASSY A., BREMER P.-T., PASCUCCI V.: Computing Morse-Smale complexes with accurate geometry. *IEEE Trans. Vis. Comput. Graph. 18*, 12 (2012), 2014–2022. doi:10.1109/TVCG.2012.209. 7

[GBPW10] GERBER S., BREMER P.-T., PASCUCCI V., WHITAKER R.: Visual exploration of high dimensional scalar functions. *IEEE Trans. Vis. Comput. Graph. 16*, 6 (2010), 1271–1280. doi:10.1109/TVCG.2010.213. 7, 8

[GDN*07] GYULASSY A., DUCHAINEAU M., NATARAJAN V., PASCUCCI V., BRINGA E., HIGGINBOTHAM A., HAMANN B.: Topologically clean distance fields. *IEEE Trans. Vis. Comput. Graph. 13*, 6 (2007), 1432–1439. doi:10.1109/TVCG.2007.70603. 8

[GGL*14] GYULASSY A., GÜNTHER D., LEVINE J. A., TIERNY J., PASCUCCI V.: Conforming Morse-Smale complexes. *IEEE Trans. Vis. Comput. Graph. 20*, 12 (2014), 2595–2603. doi:10.1109/TVCG.2014.2346434. 8

[GGTH07] GARTH C., GERHARDT F., TRICOCHE X., HAGEN H.: Efficient computation and visualization of coherent structures in fluid flow applications. *IEEE Trans. Vis. Comput. Graph. 13*, 6 (2007), 1464–1471. doi:10.1109/TVCG.2007.70551. 13

[GH83] GUCKENHEIMER J., HOLMES P.: *Nonlinear Oscillations, Dynamical Systems, and Bifurcations of Vector Fields*. Springer-Verlag, 1983. 10

[GHP*16] GUO H., HE W., PETERKA T., SHEN H. W., COLLIS S. M., HELMUS J. J.: Finite-time Lyapunov exponents and lagrangian coherent structures in uncertain unsteady flows. *IEEE Trans. Vis. Comput. Graph. 22*, 6 (2016), 1672–1682. doi:10.1109/TVCG.2016.2534560. 14

[GJR*14] GÜNTHER D., JACOBSON A., REININGHAUS J., SEIDEL H. P., SORKINE-HORNUNG O., WEINKAUF T.: Fast and memory-efficienty topological denoising of 2D and 3D scalar fields. *IEEE Trans. Vis. Comput. Graph. 20*, 12 (2014), 2585–2594. doi:10.1109/TVCG.2014.2346432. 8

[GKK*12] GYULASSY A., KOTAVA N., KIM M., HANSEN C. D., HAGEN H., PASCUCCI V.: Direct feature visualization using Morse-Smale complexes. *IEEE Trans. Vis. Comput. Graph. 18*, 9 (2012), 1549–1562. doi:10.1109/TVCG.2011.272. 8, 9

[GLL91] GLOBUS A., LEVIT C., LASINSKI T.: A tool for visualizing the topology of three-dimensional vector fields. In *IEEE Visualization* (1991), pp. 33–41. doi:10.1109/VISUAL.1991.175773. 10

[GLT*09] GARTH C., LI G.-S., TRICOCHE X., HANSEN C. D., HAGEN H.: Visualization of coherent structures in transient 2D flows. In Hege et al. [HPS09], pp. 1–13. doi:10.1007/978-3-540-88606-8_1. 13

[GNPH07] GYULASSY A., NATARAJAN V., PASCUCCI V., HAMANN B.: Efficient computation of Morse-Smale complexes for three-dimensional scalar functions. *IEEE Trans. Vis. Comput. Graph. 13*, 6 (2007), 1440–1447. doi:10.1109/TVCG.2007.70552. 7, 8

[GRSW14] GÜNTHER D., REININGHAUS J., SEIDEL H.-P., WEINKAUF T.: Notes on the simplification of the Morse-Smale complex. In Bremer et al. [BHPP14], pp. 135–150. doi:10.1007/978-3-319-04099-8_9. 8

[GST14] GÜNTHER D., SALMON J., TIERNY J.: Mandatory critical points of 2D uncertain scalar fields. *Computer Graphics Forum 33*, 3 (2014), 31–40. doi:10.1111/cgf.12359. 10

[GSW12] GÜNTHER D., SEIDEL H., WEINKAUF T.: Extraction of dominant extremal structures in volumetric data using separatrix persistence. *Computer Graphics Forum 31*, 8 (2012), 2554–2566. doi:10.1111/j.1467-8659.2012.03222.x. 8

[GTS*04a] GARTH C., TRICOCHE X., SALZBRUNN T., BOBACH T., SCHEUERMANN G.: Surface techniques for vortex visualization. In Deussen et al. [DHKS04], pp. 155–164, 346. doi:10.2312/VisSym/VisSym04/155-164. 11

[GTS04b] GARTH C., TRICOCHE X., SCHEUERMANN G.: Tracking of vector field singularities in unstructured 3D time-dependent datasets. In Rushmeier et al. [RTvW04], pp. 329–336. doi:10.1109/VISUAL.2004.107. 13

[GWT*08] GARTH C., WIEBEL A., TRICOCHE X., JOY K., SCHEUERMANN G.: Lagrangian visualization of flow-embedded surface structures. *Computer Graphics Forum* (2008). doi:10.1111/j.1467-8659.2008.01236.x. 13

[Hal02] HALLER G.: Lagrangian coherent structures from approximate velocity data. *Physics of Fluids 14*, 6 (june 2002), 1851–1861. doi:10.1063/1.1477449. 13

[HFEG15] HUETTENBERGER L., FEIGE N., EBERT A., GARTH C.: Application of Pareto sets in quality control of series production in car manufacturing. In *IEEE Pacific Visualization Symposium (PacificVis)* (2015), pp. 135–139. doi:10.1109/PACIFICVIS.2015.7156369. 17

[HG00] HAUSER H., GRÖLLER E.: Thorough insights by enhanced visualization of flow topology. In *9th International Symposium on Flow*

Visualization (2000). URL: https://www.cg.tuwien.ac.at/research/publications/2000/Hauser-2000-Tho/. 10

[HG15] HUETTENBERGER L., GARTH C.: A comparison of Pareto sets and Jacobi sets. In *Topological and Statistical Methods for Complex Data*, Bennett J., Vivodtzev F., Pascucci V., (Eds.), Mathematics and Visualization. Springer, 2015, pp. 125–141. doi:10.1007/978-3-662-44900-4_8. 17

[HH89] HELMAN J., HESSELINK L.: Representation and display of vector field topology in fluid flow data sets. *Computer 22*, 8 (1989), 27–36. doi:10.1109/2.35197. 10

[HHC*13] HUETTENBERGER L., HEINE C., CARR H., SCHEUERMANN G., GARTH C.: Towards multifield scalar topology based on Pareto optimality. *Computer Graphics Forum 32*, 3 (2013), 341–350. doi:10.1111/cgf.12121. 16

[HHG14] HUETTENBERGER L., HEINE C., GARTH C.: Decomposition and simplification of multivariate data using Pareto sets. *IEEE Trans. Vis. Comput. Graph. 20*, 12 (2014), 2684–2693. doi:10.1109/TVCG.2014.2346447. 17

[HHG16] HUETTENBERGER L., HEINE C., GARTH C.: A comparison of joint contour nets and Pareto sets. In *TopoInVis 2015* (2016). In press. 17

[HOGJ13] HUMMEL M., OBERMAIER H., GARTH C., JOY K. I.: Comparative visual analysis of Lagrangian transport in CFD ensembles. *IEEE Trans. Vis. Comput. Graph. 19*, 12 (2013), 2743–2752. doi:10.1109/TVCG.2013.141. 14

[HPS09] HEGE H.-C., POLTHIER K., SCHEUERMANN G. (Eds.): *Topology-Based Methods in Visualization II*. Mathematics and Visualization. Springer Berlin Heidelberg, 2009. 18, 19, 20, 21, 22, 23, 24, 25

[HRP*12] HARVEY W., RÜBEL O., PASCUCCI V., BREMER P.-T., WANG Y.: Enhanced topology-sensitive clustering by Reeb graph shattering. In Peikert et al. [PHCF12], pp. 77–90. doi:10.1007/978-3-642-23175-9_6. 8

[HSA*07] HLAWITSCHKA M., SCHEUERMANN G., ANWANDER A., TITTGEMEYER M., HAMANN B.: Tensor lines in tensor fields of arbitrary order. In *Advances in Visual Computing: Third International Symposium, ISVC* (Dec. 2007), Bebis G., Boyle R., Parvin B., Koracin D., Paragios N., Tanveer S.-M., Ju T., Liu Z., Coquillart S., Cruz-Neira C., Möller T., Malzbender T., (Eds.), Springer, pp. 341–350. doi:10.1007/978-3-540-76858-6_34. 15

[HSCS11] HEINE C., SCHNEIDER D., CARR H., SCHEUERMANN G.: Drawing contour trees in the plane. *IEEE Trans. Vis. Comput. Graph. 17*, 11 (2011), 1599–1611. doi:10.1109/TVCG.2010.270. 5, 6

[HSF*06] HEINE C., SCHEUERMANN G., FLAMM C., HOFACKER I. L., STADLER P. F.: Visualization of barrier tree sequences. *IEEE Trans. Vis. Comput. Graph. 12*, 5 (2006), 781–788. doi:10.1109/TVCG.2006.196. 9

[HSW11] HLAWATSCH M., SADLO F., WEISKOPF D.: Hierarchical line integration. *IEEE Trans. Vis. Comput. Graph. 17*, 8 (2011), 1148–1163. doi:10.1109/TVCG.2010.227. 13

[HVSW11] HLAWATSCH M., VOLLRATH J., SADLO F., WEISKOPF D.: Coherent structures of characteristic curves in symmetric second order tensor fields. *IEEE Transactions on Visualization and Computer Graphics 17*, 6 (2011), 781–794. doi:10.1109/TVCG.2010.107. 16

[HW10] HARVEY W., WANG Y.: Topological landscape ensembles for visualization of scalar-valued functions. *Computer Graphics Forum 29*, 3 (2010), 993–1002. doi:10.1111/j.1467-8659.2009.01706.x. 6

[IDF14] IURICICH F., DE FLORIANI L.: A combined geometrical and topological simplification hierarchy for terrain analysis. In *Proceedings of the 22nd ACM SIGSPATIAL International Conference on Advances in Geographic Information Systems* (2014), pp. 493–496. doi:10.1145/2666310.2666487. 9

[IFD15] IURICICH F., FUGACCI U., DE FLORIANI L.: Topologically-consistent simplification of discrete Morse complex. *Computers & Graphics 51* (2015), 157–166. doi:10.1016/j.cag.2015.05.007. 8

[JMC07] JOHANSSON G., MUSETH K., CARR H.: Flexible and topologically localized segmentation. In *Eurographics/IEEE-VGTC Symposium on Visualization* (2007), Museth K., Moeller T., Ynnerman A., (Eds.), The Eurographics Association, pp. 179–186. doi:10.2312/VisSym/EuroVis07/179-186. 6

[KB07] KELLER P., BERTRAM M.: Modeling and visualization of time-varying topology transitions guided by hyper Reeb graph structures. *CGIM '07 Proceedings of the Ninth IASTED International Conference on Computer Graphics and Imaging* (2007), 15–20. 9

[KER*14] KUHN A., ENGELKE W., RÖSSL C., HADWIGER M., THEISEL H.: Time line cell tracking for the approximation of Lagrangian coherent structures with subgrid accuracy. *Comput. Graph. Forum 33*, 1 (2014), 222–234. doi:10.1111/cgf.12269. 13

[KHL99] KENWRIGHT D. N., HENZE C., LEVIT C.: Feature extraction of separation and attachment lines. *IEEE Trans. Vis. Comput. Graph. 5*, 2 (1999), 135–144. doi:10.1109/2945.773805. 11

[KHNH11] KASTEN J., HOTZ I., NOACK B. R., HEGE H.-C.: On the extraction of long-living features in unsteady fluid flows. In Pascucci et al. [PTHT11], pp. 115–126. doi:10.1007/978-3-642-15014-2_10. 14

[KKW*15] KOCH S., KASTEN J., WIEBEL A., SCHEUERMANN G., HLAWITSCHKA M.: 2D vector field approximation using linear neighborhoods. *The Visual Computer* (2015), 1–16. doi:10.1007/s00371-015-1140-9. 12

[Kle04] KLEMELÄ J.: Visualization of multivariate density estimates with level set trees. *Journal of Computational and Graphical Statistics 13*, 3 (2004), 599–620. doi:10.1198/106186004X2642. 4

[KOD09] KRAUSKOPF B., OSINGA H. M., DOEDEL E. J.: Visualizing global manifolds during the transition to chaos in the Lorenz system. In Hege et al. [HPS09], pp. 115–126. doi:10.1007/978-3-540-88606-8_9. 13

[KPH*09] KASTEN J., PETZ C., HOTZ I., NOACK B. R., HEGE H.: Localized finite-time Lyapunov exponent for unsteady flow analysis. In *Proceedings of the Vision, Modeling, and Visualization Workshop 2009* (2009), Magnor M. A., Rosenhahn B., Theisel H., (Eds.), DNB, pp. 265–276. 13

[Kra10a] KRAUS M.: Visualization of uncertain contour trees. In *International Conference on Information Visualization Theory and Applications: IVAPP* (2010), Richard P., Braz J., (Eds.), Institute for Systems and Technologies of Information, Control and Communication, pp. 132–139. 10

[Kra10b] KRAUS M.: Visualizing contour trees within histograms. In *Computer Graphics and Imaging: Proceedings of the 11th IASTED International Conference on* (2010), Sappa A. D., (Ed.), ACTA Press. URL: http://www.actapress.com/Abstract.aspx?paperId=38070. 5

[KRRS14] KASTEN J., REININGHAUS J., REICH W., SCHEUERMANN G.: Toward the extraction of saddle periodic orbits. In Bremer et al. [BHPP14], pp. 55–69. doi:10.1007/978-3-319-04099-8_4. 12

[KRS03] KETTNER L., ROSSIGNAC J., SNOEYINK J.: The Safari interface for visualizing time-dependent volume data using iso-surfaces and contour spectra. *Computational Geometry 25*, 1–2 (2003), 97–116. doi:10.1016/S0925-7721(02)00132-3. 9

[KRWT12] KUHN A., RÖSSL C., WEINKAUF T., THEISEL H.: A benchmark for evaluating FTLE computations. In *IEEE Pacific Visualization Symposium* (2012), Hauser H., Kobourov S. G., Qu H., (Eds.), pp. 121–128. doi:10.1109/PacificVis.2012.6183582. 13

[LCJK*09] LARAMEE R. S., CHEN G., JANKUN-KELLY M., ZHANG E., THOMPSON D.: Bringing topology-based flow visualization to the

application domain. In Hege et al. [HPS09], pp. 161–176. `doi:10.1007/978-3-540-88606-8_12`. 10

[LG98] LÖFFELMANN H., GRÖLLER E.: Enhancing the visualization of characteristic structures in dynamical systems. In *Visualization in Scientific Computing '98: Proceedings of the Eurographics Workshop in Blaubeuren, Germany April 20–22, 1998* (Vienna, 1998), Bartz D., (Ed.), Springer Vienna, pp. 59–68. `doi:10.1007/978-3-7091-7517-0_6`. 12

[LHZP07] LARAMEE R. S., HAUSER H., ZHAO L., POST F. H.: Topology-based flow visualization, the state of the art. In *Topology-based Methods in Visualization*, Hauser H., Hagen H., Theisel H., (Eds.), Mathematics and Visualization. Springer Berlin Heidelberg, 2007, pp. 1–19. `doi:10.1007/978-3-540-70823-0_1`. 1, 10

[LJB*12] LEVINE J. A., JADHAV S., BHATIA H., PASCUCCI V., BREMER P.-T.: A quantized boundary representation of 2D flows. *Computer Graphics Forum 31*, 3pt1 (2012), 945–954. `doi:10.1111/j.1467-8659.2012.03087.x`. 11

[LMGH15] LUKASCZYK J., MACIEJEWSKI R., GARTH C., HAGEN H.: Understanding hotspots: A topological visual analytics approach. In *Proceedings of the 23rd SIGSPATIAL International Conference on Advances in Geographic Information Systems* (2015), GIS '15, ACM, pp. 1–10. `doi:10.1145/2820783.2820817`. 9

[LMW*15] LIU S., MALJOVEC D., WANG B., BREMER P.-T., PASCUCCI V.: Visualizing high-dimensional data: Advances in the past decade. In *Eurographics Conference on Visualization (EuroVis) - STARs* (2015), Borgo R., Ganovelli F., Viola I., (Eds.), The Eurographics Association, pp. 127–147. `doi:10.2312/eurovisstar.20151115`. 1

[LPG*14] LANDGE A. G., PASCUCCI V., GYULASSY A., BENNETT J. C., KOLLA H., CHEN J., BREMER P.-T.: In-situ feature extraction of large scale combustion simulations using segmented merge trees. In *High Performance Computing, Networking, Storage and Analysis, SC14: International Conference for* (2014), pp. 1020–1031. `doi:10.1109/SC.2014.88`. 4

[LWSH04] LARAMEE R. S., WEISKOPF D., SCHNEIDER J., HAUSER H.: Investigating swirl and tumble flow with a comparison of visualization techniques. In Rushmeier et al. [RTvW04], pp. 51–58. `doi:10.1109/VISUAL.2004.59`. 12

[LYL*12] LIN Z., YEH H., LARAMEE R. S., , ZHANG E.: 2D asymmetric tensor field topology. In Peikert et al. [PHCF12], pp. 191–204. `doi:10.1007/978-3-642-23175-9_13`. 15

[MBESar] MACHADO G. M., BOBLEST S., ERTL T., SADLO F.: Space-time bifurcation lines for extraction of 2D Lagrangian coherent structures. *Computer Graphics Forum 35*, 3 (to appear). 13

[MBS*04] MAHROUS K., BENNETT J., SCHEUERMANN G., HAMANN B., JOY K. I.: Topological segmentation in three-dimensional vector fields. *IEEE Trans. Vis. Comput. Graph. 10*, 2 (2004), 198–205. `doi:10.1109/TVCG.2004.1260771`. 11

[MDN12] MAADASAMY S., DORAISWAMY H., NATARAJAN V.: A hybrid parallel algorithm for computing and tracking level set topology. In *High Performance Computing (HiPC), 2012 19th International Conference on* (2012), pp. 1–10. `doi:10.1109/HiPC.2012.6507496`. 5

[MHS*96] MANDERS E. M. M., HOEBE R., STRACKEE J., VOSSEPOEL A. M., ATEN J. A.: Largest contour segmentation: A tool for the localization of spots in confocal images. *Cytometry 23*, 1 (1996), 15–21. `doi:10.1002/(SICI)1097-0320(19960101)23:1<15::AID-CYTO3>3.0.CO;2-L`. 4

[MR02] MANN S., ROCKWOOD A. P.: Computing singularities of 3D vector fields with geometric algebra. In *IEEE Visualization* (2002), pp. 283–289. `doi:10.1109/VISUAL.2002.1183786`. 11

[MS05] MASCARENHAS A., SNOEYINK J.: Implementing time-varying contour trees. *Proceedings of the twenty-first annual symposium on Computational geometry - SCG '05* (2005), 370–371. `doi:10.1145/1064092.1064151`. 9

[MS09] MASCARENHAS A., SNOEYINK J.: Isocontour based visualization of time-varying scalar fields. In *Mathematical Foundations of Scientific Visualization, Computer Graphics, and Massive Data Exploration*, Müller T., Hamann B., Russell R. D., (Eds.), Mathematics and Visualization. Springer, 2009, pp. 41–68. `doi:10.1007/b106657_3`. 1, 9

[MW13] MOROZOV D., WEBER G.: Distributed merge trees. In *Proceedings of the 18th ACM SIGPLAN Symposium on Principles and Practice of Parallel Programming* (2013), PPoPP '13, pp. 93–102. `doi:10.1145/2442516.2442526`. 4

[MW14a] MIHAI M., WESTERMANN R.: Visualizing the stability of critical points in uncertain scalar fields. *Computers & Graphics 41* (2014), 13–25. `doi:10.1016/j.cag.2014.01.007`. 10

[MW14b] MOROZOV D., WEBER G. H.: Distributed contour trees. In Bremer et al. [BHPP14], pp. 89–102. `doi:10.1007/978-3-319-04099-8_6`. 5

[MWR*16] MALJOVEC D., WANG B., ROSEN P., ALFONSI A., PASTORE G., RABITI C., PASCUCCI V.: Rethinking sensitivity analysis of nuclear simulations with topology. In *2016 IEEE Pacific Visualization Symposium (PacificVis)* (2016), pp. 64–71. `doi:10.1109/PACIFICVIS.2016.7465252`. 9

[NJS*94] NIELSON G. M., JUNG I., SRINIVASAN N., SUNG J., YOON J.: Tools for computing tangent curves and topological graphs. In *Scientific Visualization, Overviews, Methodologies, and Techniques* (1994), Nielson G. M., Hagen H., Müller H., (Eds.), IEEE Computer Society, pp. 527–562. 11

[NKWH08] NATARAJAN V., KOEHL P., WANG Y., HAMANN B.: Visual analysis of biomolecular surfaces. In *Visualization in Medicine and Life Sciences*, Linsen L., Hagen H., Hamann B., (Eds.), Mathematics and Visualization. Springer, 2008, pp. 237–255. `doi:10.1007/978-3-540-72630-2_14`. 8

[NN11] NAGARAJ S., NATARAJAN V.: Simplification of Jacobi sets. In Pascucci et al. [PTHT11], pp. 91–102. `doi:10.1007/978-3-642-15014-2_8`. 16, 17

[OGT11a] OTTO M., GERMER T., THEISEL H.: Closed stream lines in uncertain vector fields. In *Spring Conference on Computer Graphics, SCCG '11* (2011), Nishita T., Spencer S. N., (Eds.), ACM, pp. 87–94. URL: `http://dl.acm.org/citation.cfm?id=2461217`, `doi:10.1145/2461217.2461235`. 14

[OGT11b] OTTO M., GERMER T., THEISEL H.: Uncertain topology of 3D vector fields. In *IEEE Pacific Visualization Symposium* (2011), Battista G. D., Fekete J., Qu H., (Eds.), pp. 67–74. `doi:10.1109/PACIFICVIS.2011.5742374`. 14

[OHW*16] OESTERLING P., HEINE C., WEBER G. H., MOROZOV D., SCHEUERMANN G.: Computing and visualizing time-varying merge trees for high-dimensional data. In *TopoInVis 2015* (2016), Springer. In press. 9

[OHWS13] OESTERLING P., HEINE C., WEBER G. H., SCHEUERMANN G.: Visualizing nD point clouds as topological landscape profiles to guide local data analysis. *IEEE Trans. Vis. Comput. Graph. 19*, 3 (2013), 514–526. `doi:10.1109/TVCG.2012.120`. 4

[OST*10] OESTERLING P., SCHEUERMANN G., TERESNIAK S., HEYER G., KOCH S., ERTL T., WEBER G.: Two-stage framework for a topology-based projection and visualization of classified document collections. In *Visual Analytics Science and Technology (VAST), 2010 IEEE Symposium on* (2010), pp. 91–98. `doi:10.1109/VAST.2010.5652940`. 4, 6

[Par13] PARSA S.: A deterministic $O(m\log m)$ time algorithm for the Reeb graph. *Discrete & Computational Geometry 49*, 4 (2013), 864–878. `doi:10.1007/s00454-013-9511-3`. 5

[PCM03] PASCUCCI V., COLE-MCLAUGHLIN K.: Parallel computation of the topology of level sets. *Algorithmica 38*, 1 (2003), 249–268. `doi:10.1007/s00453-003-1052-3`. 5

[PCMS04] PASCUCCI V., COLE-MCLAUGHLIN K., SCORZELLI

G.: Multi-resolution computation and presentation of contour trees. In *Proceedings of IASTED Conference on Visualization, Imaging, and Image Processing* (2004), pp. 452–290. URL: http://citeseerx.ist.psu.edu/viewdoc/summary?doi=10.1.1.308.8105&rank=1. 5, 6

[PD10] PEACOCK T., DABIRI J.: Introduction to focus issue: Lagrangian coherent structures. *Chaos 20*, 1 (2010). doi:10.1063/1.3278173. 13

[PHCF12] PEIKERT R., HAUSER H., CARR H., FUCHS R. (Eds.): *Topological Methods in Data Analysis and Visualization II*. Mathematics and Visualization. Springer Berlin Heidelberg, 2012. 21, 22, 23, 25

[PLC*11] PALKE D., LIN Z., CHEN G., YEH H., VINCENT P., LARAMEE R., ZHANG E.: Asymmetric tensor field visualization for surfaces. *IEEE Trans. Vis. Comput. Graph. 17*, 12 (2011), 1979–1988. doi:10.1109/TVCG.2011.170. 16

[PPF*11] POBITZER A., PEIKERT R., FUCHS R., SCHINDLER B., KUHN A., THEISEL H., MATKOVIÄĞ K., HAUSER H.: The state of the art in topology-based visualization of unsteady flow. *Computer Graphics Forum 30*, 6 (2011), 1789–1811. doi:10.1111/j.1467-8659.2011.01901.x. 10

[PPH12] PETZ C., PÖTHKOW K., HEGE H.-C.: Probabilistic local features in uncertain vector fields with spatial correlation. *Computer Graphics Forum 31*, 3pt2 (2012), 1045–1054. doi:10.1111/j.1467-8659.2012.03097.x. 14

[PRJ12] POTTER K., ROSEN P., JOHNSON C. R.: From quantification to visualization: A taxonomy of uncertainty visualization approaches. In *Uncertainty Quantification in Scientific Computing: 10th IFIP WG 2.5 Working Conference, WoCoUQ 2011, Boulder, CO, USA, August 1-4, 2011, Revised Selected Papers* (Berlin, Heidelberg, 2012), Dienstfrey A. M., Boisvert R. F., (Eds.), Springer Berlin Heidelberg, pp. 226–249. doi:10.1007/978-3-642-32677-6_15. 14

[PS07] PEIKERT R., SADLO F.: Visualization methods for vortex rings and vortex breakdown bubbles. In *EuroVis07: Joint Eurographics - IEEE VGTC Symposium on Visualization* (2007), Museth K., Möller T., Ynnerman A., (Eds.), Eurographics Association, pp. 211–218. doi:10.2312/VisSym/EuroVis07/211-218. 11, 12

[PS09] PEIKERT R., SADLO F.: Flow topology beyond skeletons: Visualization of features in recirculating flow. In Hege et al. [HPS09], pp. 145–160. doi:10.1007/978-3-540-88606-8_11. 12

[PSBM07] PASCUCCI V., SCORZELLI G., BREMER P.-T., MASCARENHAS A.: Robust on-line computation of Reeb graphs: Simplicity and speed. *ACM Transactions on Graphics 26*, 3 (2007). doi:10.1145/1276377.1276449. 5

[PTHT11] PASCUCCI V., TRICOCHE X., HAGEN H., TIERNY J. (Eds.): *Topological Methods in Data Analysis and Visualization*. Mathematics and Visualization. Springer Berlin Heidelberg, 2011. 21, 22, 23, 25

[PVH*03] POST F. H., VROLIJK B., HAUSER H., LARAMEE R. S., DOLEISCH H.: The state of the art in flow visualisation: Feature extraction and tracking. *Computer Graphics Forum 22*, 4 (2003), 775–792. doi:10.1111/j.1467-8659.2003.00723.x. 1

[Ree46] REEB G.: Sur les points singuliers d'une forme de Pfaff completement intégrable ou d'une fonction numérique. *Computes Rendus de L'Académie des Séances, Paris 222*, 847–849 (1946). 3

[RH11] REININGHAUS J., HOTZ I.: Combinatorial 2D vector field topology extraction and simplification. In Pascucci et al. [PTHT11], pp. 103–114. doi:10.1007/978-3-642-15014-2_9. 11, 12

[RKG*11] REININGHAUS J., KOTAVA N., GUENTHER D., KASTEN J., HAGEN H., HOTZ I.: A scale space based persistence measure for critical points in 2D scalar fields. *IEEE Trans. Vis. Comput. Graph. 17*, 12 (2011), 2045–2052. doi:10.1109/TVCG.2011.159. 8

[RKWH12] REININGHAUS J., KASTEN J., WEINKAUF T., HOTZ I.: Efficient computation of combinatorial feature flow fields. *IEEE Trans. Vis. Comput. Graph. 18*, 9 (2012), 1563–1573. doi:10.1109/TVCG.2011.269. 9

[RL14] RIECK B., LEITTE H.: Structural analysis of multivariate point clouds using simplicial chains. *Computer Graphics Forum 33*, 8 (2014), 28–37. doi:10.1111/cgf.12398. 3

[RL15] RIECK B., LEITTE H.: Persistent homology for the evaluation of dimensionality reduction schemes. *Computer Graphics Forum 34*, 3 (2015), 431–440. doi:10.1111/cgf.12655. 3

[RML12] RIECK B., MARA H., LEITTE H.: Multivariate data analysis using persistence-based filtering and topological signatures. *IEEE Trans. Vis. Comput. Graph. 18*, 12 (2012), 2382–2391. doi:10.1109/TVCG.2012.248. 3

[RS14] RAICHEL B., SESHADHRI C.: Avoiding the global sort: A faster contour tree algorithm. *ArXiv e-prints* (2014). arXiv:1411.2689. 5

[RSH*12] REICH W., SCHNEIDER D., HEINE C., WIEBEL A., CHEN G., SCHEUERMANN G.: Combinatorial vector field topology in three dimensions. In Peikert et al. [PHCF12], pp. 47–59. doi:10.1007/978-3-642-23175-9_4. 10

[RT12] RÖSSL C., THEISEL H.: Streamline embedding for 3D vector field exploration. *IEEE Trans. Vis. Comput. Graph. 18*, 3 (2012), 407–420. doi:10.1109/TVCG.2011.78. 12

[RTvW04] RUSHMEIER H., TURK G., VAN WIJK J. J. (Eds.):. *15th IEEE Visualization 2004 Conference (VIS 2004)* (2004), IEEE Computer Society. 20, 22, 24

[RWS11] ROBINS V., WOOD P. J., SHEPPARD A. P.: Theory and algorithms for constructing discrete Morse complexes from grayscale digital images. *IEEE Trans. on Pattern Analysis and Machine Intelligence 33*, 8 (2011), 1646–1658. doi:10.1109/TPAMI.2011.95. 7, 8

[SB06] SOHN B.-S., BAJAJ C.: Time-varying contour topology. *IEEE Trans. Vis. Comput. Graph. 12*, 1 (2006), 14–25. doi:10.1109/TVCG.2006.16. 9

[SB12] SZYMCZAK A., BRUNHART-LUPO N.: Nearly recurrent components in 3D piecewise constant vector fields. *Computer Graphics Forum 31*, 3 (2012), 1115–1124. doi:10.1111/j.1467-8659.2012.03104.x. 12

[Sch11] SCHULZ T.: Topological features in 2D symmetric higher-order tensor fields. *Computer Graphics Forum 30*, 3 (2011), 841–850. doi:10.1111/j.1467-8659.2011.01933.x. 15, 16

[SCT*10] SANDERSON A., CHEN G., TRICOCHE X., PUGMIRE D., KRUGER S., BRESLAU J.: Analysis of recurrent patterns in toroidal magnetic fields. *IEEE Trans. Vis. Comput. Graph. 16*, 6 (2010), 1431–1440. doi:10.1109/TVCG.2010.133. 12

[SFRS12] SCHNEIDER D., FUHRMANN J., REICH W., SCHEUERMANN G.: A variance based FTLE-like method for unsteady uncertain vector fields. In Peikert et al. [PHCF12], pp. 255–268. doi:10.1007/978-3-642-23175-9_17. 14

[SHCS13] SCHNEIDER D., HEINE C., CARR H., SCHEUERMANN G.: Interactive comparison of multifield scalar data based on largest contours. *Computer Aided Geometric Design 30*, 6 (2013), 521–528. Foundations of Topological Analysis. doi:10.1016/j.cagd.2012.03.023. 16

[SHK*97] SCHEUERMANN G., HAGEN H., KRÜGER H., MENZEL M., ROCKWOOD A. P.: Visualization of higher order singularities in vector fields. In *IEEE Visualization* (1997), pp. 67–74. doi:10.1109/VISUAL.1997.663858. 11

[SK91] SHINAGAWA Y., KUNII T.: Constructing a Reeb graph automatically from cross sections. *Computer Graphics and Applications, IEEE 11*, 6 (1991), 44–51. doi:10.1109/38.103393. 4, 5

[SKK91] SHINAGAWA Y., KUNII T., KERGOSIEN Y.: Surface coding based on Morse theory. *Computer Graphics and Applications, IEEE 11*, 5 (1991), 66–78. doi:10.1109/38.90568. 5

[SKMR98] SCHEUERMANN G., KRÜGER H., MENZEL M., ROCKWOOD A.: Visualizing nonlinear vector field topology. *IEEE Trans. Vis. Comput. Graph. 4*, 2 (1998), 109–116. doi:10.1109/2945.694953. 11

[SLM05] SHADDEN S., LEKIEN F., MARSDEN J.: Definition and properties of Lagrangian coherent structures from finit-time Lyapunov exponents in two-dimensional aperiodic flows. *Physica D 212* (2005), 271–304. `doi:10.1016/j.physd.2005.10.007`. 13

[SMC07] SINGH G., MÈMOLI F., CARLSSON G.: Topological methods for the analysis of high dimensional data sets and 3D object recognition. In *Eurographics Symposium on Point-Based Graphics* (2007), Botsch M., Pajarola R., Chen B., Zwicker M., (Eds.), The Eurographics Association, pp. 91–100. `doi:10.2312/SPBG/SPBG07/091-100`. 16

[SMN12] SHIVASHANKAR N., MAADASAMY S., NATARAJAN V.: Parallel computation of 2D Morse-Smale complexes. *IEEE Trans. Vis. Comput. Graph. 18*, 10 (2012), 1757–1770. `doi:10.1109/TVCG.2011.284`. 7

[SN12] SHIVASHANKAR N., NATARAJAN V.: Parallel computation of 3D Morse-Smale complexes. *Computer Graphics Forum 31*, 3pt1 (2012), 965–974. `doi:10.1111/j.1467-8659.2012.03089.x`. 7

[SP07] SADLO F., PEIKERT R.: Efficient visualization of Lagrangian coherent structures by filtered AMR ridge extraction. *IEEE Trans. Vis. Comput. Graph. 13*, 6 (2007), 1456–1463. `doi:10.1109/TVCG.2007.70554`. 13

[SP09] SADLO F., PEIKERT R.: Visualizing Lagrangian coherent structures and comparison to vector field topology. In Hege et al. [HPS09], pp. 15–29. `doi:10.1007/978-3-540-88606-8_2`. 13

[SRW*16] SKRABA P., ROSEN P., WANG B., CHEN G., BHATIA H., PASCUCCI V.: Critical point cancellation in 3D vector fields: Robustness and discussion. *IEEE Trans. Vis. Comput. Graph. 22*, 6 (2016), 1683–1693. `doi:10.1109/TVCG.2016.2534538`. 12

[SRWS10] SCHNEIDER D., REICH W., WIEBEL A., SCHEUERMANN G.: Topology aware stream surfaces. *Computer Graphics Forum 29*, 3 (2010), 1153–1161. `doi:10.1111/j.1467-8659.2009.01672.x`. 11

[SSZC94] SAMTANEY R., SILVER D., ZABUSKY N., CAO J.: Visualizing features and tracking their evolution. *Computer 27*, 7 (1994), 20–27. `doi:10.1109/2.299407`. 9

[STS07] SCHULTZ T., THEISEL H., SEIDL H.-P.: Topological visualization of brain diffusion MRI data. *IEEE Trans. Vis. Comput. Graph. 13*, 6 (2007), 1496–1503. `doi:10.1109/TVCG.2007.70602`. 15

[SW10] SADLO F., WEISKOPF D.: Time-dependent 2-D vector field topology: An approach inspired by Lagrangian coherent structures. *Computer Graphics Forum 29*, 1 (2010), 88–100. `doi:10.1111/j.1467-8659.2009.01546.x`. 14

[SWC*08] SCHNEIDER D., WIEBEL A., CARR H., HLAWITSCHKA M., SCHEUERMANN G.: Interactive comparison of scalar fields based on largest contours with applications to flow visualization. *IEEE Trans. Vis. Comput. Graph. 14*, 6 (2008), 1475–1482. `doi:10.1109/TVCG.2008.143`. 16

[SWCR15] SKRABA P., WANG B., CHEN G., ROSEN P.: Robustness-based simplification of 2d steady and unsteady vector fields. *IEEE Trans. Vis. Comput. Graph. 21*, 8 (2015), 930–944. `doi:10.1109/TVCG.2015.2440250`. 13

[SZ12] SZYMCZAK A., ZHANG E.: Robust Morse decompositions of piecewise constant vector fields. *IEEE Trans. Vis. Comput. Graph. 18*, 6 (2012), 938–951. `doi:10.1109/TVCG.2011.88`. 12

[Szy05] SZYMCZAK A.: Subdomain aware contour trees and contour evolution in time-dependent scalar fields. In *Shape Modeling and Applications, 2005 International Conference* (2005), pp. 136–144. `doi:10.1109/SMI.2005.45`. 9

[Szy11] SZYMCZAK A.: Stable Morse decompositions for piecewise constant vector fields on surfaces. *Computer Graphics Forum 30*, 3 (2011), 851–860. `doi:10.1111/j.1467-8659.2011.01934.x`. 14

[TFO09] TAKAHASHI S., FUJISHIRO I., OKADA M.: Applying manifold learning to plotting approximate contour trees. *IEEE Trans. Vis.*

[TGK*04] TRICOCHE X., GARTH C., KINDLMANN G. L., DEINES E., SCHEUERMANN G., RÜTTEN M., HANSEN C. D.: Visualization of intricate flow structures for vortex breakdown analysis. In Rushmeier et al. [RTvW04], pp. 187–194. `doi:10.1109/VISUAL.2004.113`. 12

[TGS11] TRICOCHE X., GARTH C., SANDERSON A. R.: Visualization of topological structures in area-preserving maps. *IEEE Trans. Vis. Comput. Graph. 17*, 12 (2011), 1765–1774. `doi:10.1109/TVCG.2011.254`. 12

[THBG12] TRICOCHE X., HLAWITSCHKA M., BARAKAT S., GARTH C.: Beyond topology: A Lagrangian metaphor to visualize the structure of 3D tensor fields. In *New Developments in the Visualization and Processing of Tensor Fields*, Laidlaw D. H., Vilanova A., (Eds.). Springer, 2012, pp. 93–110. `doi:10.1007/978-3-642-27343-8`. 15, 16

[TIS*95] TAKAHASHI S., IKEDA T., SHINAGAWA Y., KUNII T. L., UEDA M.: Algorithms for extracting correct critical points and constructing topological graphs from discrete geographical elevation data. *Computer Graphics Forum 14*, 3 (1995), 181–192. `doi:10.1111/j.1467-8659.1995.cgf143_0181.x`. 5

[TN11] THOMAS D. M., NATARAJAN V.: Symmetry in scalar field topology. *IEEE Trans. Vis. Comput. Graph. 17*, 12 (2011), 2035–2044. `doi:10.1109/TVCG.2011.236`. 5, 6

[TN13] THOMAS D. M., NATARAJAN V.: Detecting symmetry in scalar fields using augmented extremum graphs. *IEEE Trans. Vis. Comput. Graph. 19*, 12 (2013), 2663–2672. `doi:10.1109/TVCG.2013.148`. 9

[TRS03a] THEISEL H., RÖSSL C., SEIDEL H.: Combining topological simplification and topology preserving compression for 2D vector fields. In *11th Pacific Conference on Computer Graphics and Applications (PG 2003)* (2003), pp. 419–423. `doi:10.1109/PCCGA.2003.1238287`. 12

[TRS03b] THEISEL H., RÖSSL C., SEIDEL H.: Using feature flow fields for topological comparison of vector fields. In *Proceedings of the Vision, Modeling, and Visualization Conference 2003 (VMV 2003)* (2003), Ertl T., (Ed.), Aka GmbH, pp. 521–528. 14

[TS03] THEISEL H., SEIDEL H.-P.: Feature flow fields. In *Proc. Symposium on Data Visualisation 2003* (2003), VISSYM '03, Eurographics Association, pp. 141–148. URL: `http://wwwisg.cs.uni-magdeburg.de/visual/files/publications/Archive/Theisel_2003_VisSym.pdf`. 13

[TSH00] TRICOCHE X., SCHEUERMANN G., HAGEN H.: A topology simplification method for 2D vector fields. In *IEEE Visualization* (2000), pp. 359–366. `doi:10.1109/VISUAL.2000.885716`. 12

[TSH01a] TRICOCHE X., SCHEUERMANN G., HAGEN H.: Continuous topology simplification of planar vector fields. In *IEEE Visualization 2001* (2001), Ertl T., Joy K. I., Varshney A., (Eds.), pp. 159–166. `doi:10.1109/VISUAL.2001.964507`. 12

[TSH01b] TRICOCHE X., SCHEUERMANN G., HAGEN H.: Tensor topology tracking: A visualization method for time-dependent 2D symmetric tensor fields. *Computer Graphics Forum 20*, 3 (2001), 461–470. `doi:10.1111/1467-8659.00539`. 15

[TSHC01] TRICOCHE X., SCHEUERMANN G., HAGEN H., CLAUSS S.: Vector and tensor field topology simplification on irregular grids. In *Proceedings of the 2001 Joint Eurographics and IEEE TCVG Symposium on Visualization* (2001), Ebert D. S., Favre J. M., Peikert R., (Eds.), VisSym 2001, Eurographics Association, pp. 107–116. `doi:10.1007/978-3-7091-6215-6_12`. 12, 15

[TTF04] TAKAHASHI S., TAKESHIMA Y., FUJISHIRO I.: Topological volume skeletonization and its application to transfer function design. *Graphical Models 66*, 1 (2004), 24–49. `doi:10.1016/j.gmod.2003.08.002`. 6

Comput. Graph. 15, 6 (2009), 1185–1192. `doi:10.1109/TVCG.2009.119`. 5

[TWHS03] THEISEL H., WEINKAUF T., HEGE H., SEIDEL H.: Saddle connectors - an approach to visualizing the topological skeleton of complex 3D vector fields. In *14th IEEE Visualization 2003 Conference (VIS 2003)* (2003), Turk G., van Wijk J. J., Moorhead II R. J., (Eds.), pp. 225–232. doi:10.1109/VISUAL.2003.1250376. 11

[TWHS04] THEISEL H., WEINKAUF T., HEGE H.-C., SEIDEL H.-P.: Grid-independent detection of closed stream lines in 2D vector fields. In *Proc. Vision, Modeling and Visualization* (2004), pp. 421–428. 12

[TWHS05] THEISEL H., WEINKAUF T., HEGE H., SEIDEL H.: Topological methods for 2D time-dependent vector fields based on stream lines and path lines. *IEEE Trans. Vis. Comput. Graph. 11*, 4 (2005), 383–394. doi:10.1109/TVCG.2005.68. 13

[TWSH02] TRICOCHE X., WISCHGOLL T., SCHEUERMANN G., HAGEN H.: Topology tracking for the visualization of time-dependent two-dimensional flows. *Computers & Graphics 26*, 2 (2002), 249–257. doi:10.1016/S0097-8493(02)00056-0. 13

[UMW*12] USHIZIMA D., MOROZOV D., WEBER G., BIANCHI A., SETHIAN J., BETHEL W.: Augmented topological descriptors of pore networks for material science. *IEEE Trans. Vis. Comput. Graph. 18*, 12 (2012), 2041–2050. doi:10.1109/TVCG.2012.200. 5

[ÜSE13] ÜFFINGER M., SADLO F., ERTL T.: A time-dependent vector field topology based on streak surfaces. *IEEE Trans. Vis. Comput. Graph. 19*, 3 (2013), 379–392. doi:10.1109/TVCG.2012.131. 14

[vKvOB*97] VAN KREVELD M., VAN OOSTRUM R., BAJAJ C., PASCUCCI V., SCHIKORE D.: Contour trees and small seed sets for isosurface traversal. In *Proceedings of the Thirteenth Annual Symposium on Computational Geometry* (1997), SCG '97, ACM, pp. 212–220. doi:10.1145/262839.269238. 6

[VMH*13] VOLKE S., MIDDENDORF M., HLAWITSCHKA M., KASTEN J., ZECKZER D., SCHEUERMANN G.: dPSO-vis: Topology-based visualization of discrete particle swarm optimization. *Computer Graphics Forum 32*, 3pt3 (2013), 351–360. doi:10.1111/cgf.12122. 4

[WBD*11] WEBER G., BREMER P.-T., DAY M., BELL J., PASCUCCI V.: Feature tracking using Reeb graphs. In Pascucci et al. [PTHT11], pp. 241–253. doi:10.1007/978-3-642-15014-2_20. 5

[WBP07] WEBER G., BREMER P.-T., PASCUCCI V.: Topological landscapes: A terrain metaphor for scientific data. *IEEE Trans. Vis. Comput. Graph. 13*, 6 (2007), 1416–1423. doi:10.1109/TVCG.2007.70601. 5, 6

[WBP12] WEBER G. H., BREMER P.-T., PASCUCCI V.: Topological cacti: Visualizing contour-based statistics. In Peikert et al. [PHCF12], pp. 63–76. doi:10.1007/978-3-642-23175-9_5. 6

[WCBP12] WIDANAGAMAACHCHI W., CHRISTENSEN C., BREMER P.-T., PASCUCCI V.: Interactive exploration of large-scale time-varying data using dynamic tracking graphs. In *Large Data Analysis and Visualization (LDAV), 2012 IEEE Symposium on* (2012), pp. 9–17. doi:10.1109/LDAV.2012.6378962. 9

[WDC*07] WEBER G. H., DILLARD S. E., CARR H., PASCUCCI V., HAMANN B.: Topology-controlled volume rendering. *IEEE Trans. Vis. Comput. Graph. 13*, 2 (2007), 330–341. doi:10.1109/TVCG.2007.47. 6

[WGS07] WIEBEL A., GARTH C., SCHEUERMANN G.: Computation of localized flow for steady and unsteady vector fields and its applications. *IEEE Trans. Vis. Comput. Graph. 13*, 4 (2007), 641–651. doi:10.1109/TVCG.2007.4293009. 11

[WGS10] WEINKAUF T., GINGOLD Y., SORKINE O.: Topology-based smoothing of 2D scalar fields with C^1-continuity. *Computer Graphics Forum 29*, 3 (2010), 1221–1230. doi:10.1111/j.1467-8659.2009.01702.x. 8

[WIFDF13] WEISS K., IURICICH F., FELLEGARA R., DE FLORIANI L.: A primal/dual representation for discrete Morse complexes on tetrahedral meshes. *Computer Graphics Forum 32*, 3pt3 (2013), 361–370. doi:10.1111/cgf.12123. 7

[WRKS10] WIEBEL A., REICH W., KOCH S., SCHEUERMANN G.: Vector field topology in the context of separation and attachment of flows. In *Foundations of Topological Analysis Workshop* (2010). Co-located with IEEE VisWeek 2010. 11

[WRS*13] WANG B., ROSEN P., SKRABA P., BHATIA H., PASCUCCI V.: Visualizing robustness of critical points for 2D time-varying vector fields. *Computer Graphics Forum 32*, 3pt2 (2013), 221–230. doi:10.1111/cgf.12109. 13

[WS01] WISCHGOLL T., SCHEUERMANN G.: Detection and visualization of closed streamlines in planar flows. *IEEE Trans. Vis. Comput. Graph. 7*, 2 (2001), 165–172. doi:10.1109/2945.928168. 12

[WS02] WISCHGOLL T., SCHEUERMANN G.: Locating closed streamlines in 3D vector fields. In *Proceedings of the 2002 Joint Eurographics and IEEE TCVG Symposium on Visualization, VisSym 2002* (2002), Ebert D. S., Brunet P., Navazo I., (Eds.), Eurographics Association, pp. 227–232. doi:10.2312/VisSym/VisSym02/227-232. 12

[WSH01] WISCHGOLL T., SCHEUERMANN G., HAGEN H.: Tracking closed streamlines in time dependent planar flows. In *Proceedings of the Vision Modeling and Visualization Conference 2001 (VMV-01)* (2001), Ertl T., Girod B., Niemann H., Seidel H., (Eds.), Aka GmbH, pp. 447–454. 13

[WTGP11] WEINKAUF T., THEISEL H., GELDER A. V., PANG A.: Stable feature flow fields. *IEEE Trans. Vis. Comput. Graph. 17*, 6 (2011), 770–780. doi:10.1109/TVCG.2010.93. 13

[WTHS04a] WEINKAUF T., THEISEL H., HEGE H., SEIDEL H.: Boundary switch connectors for topological visualization of complex 3D vector fields. In Deussen et al. [DHKS04], pp. 183–192. doi:10.2312/VisSym/VisSym04/183-192. 11

[WTHS04b] WEINKAUF T., THEISEL H., HEGE H.-C., SEIDEL H.-P.: Topological construction and visualization of higher order 3d vector fields. *Computer Graphics Forum 23*, 3 (2004), 469–478. doi:10.1111/j.1467-8659.2004.00778.x. 11

[WTS*05] WEINKAUF T., THEISEL H., SHI K., HEGE H.-C., SEIDEL H.-P.: Extracting higher order critical points and topological simplification of 3D vector fields. In *Proceedings IEEE Visualization 2005* (2005), pp. 559–566. 12

[WTS09] WIEBEL A., TRICOCHE X., SCHEUERMANN G.: Extraction of separation manifolds using topological structures in flow cross sections. In Hege et al. [HPS09], pp. 31–43. doi:10.1007/978-3-540-88606-8_3. 12

[WWL16] WANG W., WANG W., LI S.: From numerics to combinatorics: a survey of topological methods for vector field visualization. *Journal of Visualization* (2016), 1–26. doi:10.1007/s12650-016-0348-8. 1, 10

[WZ13] WU K., ZHANG S.: A contour tree based visualization for exploring data with uncertainty. *International Journal for Uncertainty Quantification 3*, 3 (2013), 203–223. doi:10.1615/Int.J.UncertaintyQuantification.2012003956. 10

[YKP05] YE X., KAO D., PANG A.: Strategy for seeding 3D streamlines. In *16th IEEE Visualization Conference (VIS 2005)* (2005), pp. 60–. doi:10.1109/VIS.2005.92. 12

[ZAM15] ZHANG W., AGARWAL P. K., MUKHERJEE S.: Contour trees of uncertain terrains. In *Proceedings of the 23rd SIGSPATIAL International Conference on Advances in Geographic Information Systems* (2015), GIS '15, ACM, pp. 43:1–10. doi:10.1145/2820783.2820823. 10

[ZP04] ZHENG X., PANG A.: Topological lines in 3D tensor fields. In *Proceedings of the IEEE Conference on Visualization '04* (2004), VIS '04, pp. 313–320. doi:10.1109/VISUAL.2004.105. 15

[ZPP05] ZHENG X., PARLETT B., PANG A.: Topological lines in 3D tensor fields and discriminant Hessian factorization. *IEEE Trans. Vis. Comput. Graph. 11*, 4 (2005), 395–407. doi:10.1109/TVCG.2005.67. 15